Emre BEŞKAZAK COLLOIDAL PEROVSKITE NANOCYRISTALS AND LED APPLICATIONS AGU 2019

# COLLOIDAL PEROVSKITE NANOCRYSTALS AND LED APPLICATIONS

A THESIS
SUBMITTED TO THE DEPARTMENT OF ELECTRICAL AND COMPUTER ENGINEERING
AND THE GRADUATE SCHOOL OF ENGINEERING AND SCIENCE
OF ABDULLAH GUL UNIVERSITY
IN PARTIAL FULFILLMENT OF THE REQUIREMENTS
FOR THE DEGREE OF
M.Sc.

By
Emre BEŞKAZAK
December 2019

# COLLOIDAL PEROVSKITE NANOCRYSTALS AND LED APPLICATIONS

A THESIS
SUBMITTED TO THE DEPARTMENT OF ELECTRICAL AND COMPUTER ENGINEERING
AND THE GRADUATE SCHOOL OF ENGINEERING AND SCIENCE OF ABDULLAH GUL UNIVERSITY
IN PARTIAL FULFILLMENT OF THE REQUIREMENTS
FOR THE DEGREE OF
M. Sc.

By
Emre BEŞKAZAK
December 2019

## SCIENTIFIC ETHICS COMPLIANCE

I hereby declare that all information in this document has been obtained in accordance with academic rules and ethical conduct. I also declare that, as required by these rules and conduct, I have fully cited and referenced all materials and results that are not original to this work.

Name-Surname: Emre BEŞKAZAK

Signature :

**REGULATORY COMPLIANCE**

M.Sc. thesis titled Colloidal Perovskite Nano Crystals And LED Applications has been prepared in accordance with the Thesis Writing Guidelines of the Abdullah Gül University, Graduate School of Engineering & Science.

Prepared By

Emre BEŞKAZAK

Advisor

Assoc. Prof. Evren MUTLUGÜN

Head of the Electrical and Computer Engineering Program

Assoc. Prof. Vehbi Çağrı GÜNGÖR

## ACCEPTANCE AND APPROVAL

M.Sc. thesis titled Colloidal Perovskite Nano Crystals And LED Applications and prepared by Emre BEŞKAZAK has been accepted by the jury in the Electrical and Computer Engineering Graduate Program at Abdullah Gül University, Graduate School of Engineering & Science.

26 /12 / 2019

**JURY:**

Advisor : Assoc. Prof. Evren MUTLUGÜN

Member : Assoc. Prof. Mustafa Serdar ÖNSES

Member : Asst. Prof. Talha ERDEM

**APPROVAL:**

The acceptance of this M.Sc. thesis has been approved by the decision of the Abdullah Gül University, Graduate School of Engineering & Science, Executive Board dated ….. /….. / …….. and numbered ……..……. .

…….. /…….. / ……..

Graduate School Dean

Prof. İrfan ALAN

# ABSTRACT

# COLLOIDAL PEROVSKITE NANOCRYSTALS AND LED APPLICATIONS

Emre BEŞKAZAK
MSc. in Electrical and Computer Engineering
**Supervisor:** Assoc. Prof. Evren MUTLUGÜN

December 2019

Colloidal perovskite nanocrystals, recently, attracted a great amount of research interest because of their near-unity photoluminescence quantum yield efficiency, narrow emission linewidth, easy tunability of wavelength covering full visible spectrum thanks to quantum confinement effect and halogen composition dependence, as well as the compatibility with the flexible substrates. All these properties make colloidal perovskite nanocrystals a serious candidate for use as emissive layers in next-generation light-emitting diodes (LEDs) and displays. In this thesis, syntheses of colloidal nanocrystals were demonstrated, and red and green light-emitting diodes which contain perovskite nanocrystals as emissive layer were fabricated, optimized, and measured. The main challenges of perovskite nanocrystals based light-emitting diode applications are identified, such as stability and toxicity. Additionally, blue and green light-emitting diodes which employ CdSe based semiconductor nanocrystals as emissive layer were fabricated on ITO coated PET (Polyethylene terephthalate) and glass substrates. A flexible white LED is presented as a proof of concept, by fixing a flexible polymer layer consists of red and green InP based semiconductor nanocrystals on top of the CdSe based blue LED.

*Keywords: colloidal, perovskite, nanocrystals, quantum dots, light-emitting diodes, QLED*

# ÖZET

# KOLOİDAL PEROVSKİT NANOKRİSTALLER VE IŞIK SAÇAN DİYOT UYGULAMALARI

Emre BEŞKAZAK
Elektrik ve Bilgisayar Mühendisliği Bölümü Yüksek Lisans
Tez Yöneticisi: Doç. Dr. Evren MUTLUGÜN
Kasım-2019

Koloidal perovskit nano kristaller yakın zaman içinde, büyük miktarda bilimsel ilgi çekti. Neredeyse %100 fotolüminesans kuantum ışıma verimliliği, dar bir ışıma dalga boyuna sahip olmaları, ışıma dalga boylarının tüm gözle görülür spekturumu kapsaması, ışıma dalga boyu ayarının parçacık boyutuna ve daha da önemlisi halojen bileşimine bağlı olarak kolayca ayarlanabilmesi ve esnek cihaz tasarımlarına uygunluğu bu ilginin sebeplerini oluşturmaktadır. Tüm bu sayılan özellikler perovskit nano kristalleri gelecekteki yeni nesil ışık saçan diyot uygulamaları ve ekran teknolojilerinde kullanılmak üzere ciddi bir aday yapmaktadır. Bu tez kapsamında, kolloidal nano kristallerin sentezi gösterilmiş ve ışıyan tabakalarında perovskit nano kristaller bulunan kırmızı ve yeşil ışık saçan diyotlar (LED'ler) üretilmiş, optimize edilmiş ve ölçülmüştür. Deneylerden elde edilen sonuçlar üzerine perovskit nano kristallerin ışık saçan diyot uygulamalarında karşılaşılan temel sorunlar ve endişeler tanımlanmıştır. Ayrıca ışıyan tabakalarında CdSe tabanlı yarı iletken nano kristal bulunduran yeşil ve mavi LED'ler ITO kaplı PET (Polyethylene terephthalate) ve cam tabanlar üzerinde üretilmiştir. Kavramsal gösterim amacıyla esnek beyaz LED üretilmiştir. Bunun için, üzeri renk değişim katmanı olarak kırmızı ve yeşil InP tabanlı yarı iletken nano kristaller içeren esnek polimer ile kaplı, esnek bir CdSe tabanlı mavi LED kullanılmıştır.

*Anahtar kelimeler: Koloidal, perovskite, nano kristaller, kuantum noktacıklar, ışık saçan diyotlar, QLED*

# Acknowledgements

I would like to express my sincere gratitude to my research advisor Associate Professor Evren MUTLUGÜN for his endless support and guidance during my study. His wisdom will guide me throughout my life.

I would like to thank Mutlugün Research Group Members Yemliha Altıntas, Miray Ünlü Yazıcı, Ahmet Faruk Yazıcı, Sinan Genç, Eren Uzuner, Kaan Elmacıoğlu for their companionship and support.

I would like to acknowledge the support and grant of TÜBİTAK projects numbered 114E107 and 117E239, and the Turkish Academy of Sciences The Young Scientists Award Program (TUBA-GEBIP 2017).

Finally, I would like to thank my dear family for their continuous and irreplaceable support.

# Table Of Contents

# List of Figures

# List of Tables

# Chapter 1

# Introduction

## 1.1 Introduction to Semiconductor Nanocrystals (Quantum Dots)

It has been more than three decades since the exotic quantum size effects of semiconductor nanocrystals were discovered [1–3]. Before the discovery, semiconductors were known for their constant energy gap between the valence band and the conduction band. The width of the band gap determines the optical properties of a semiconductor material such as luminescence and absorption spectrums. The only way to engineer the band gap of a bulk semiconductor was to control the composition of the material. However, if the size of a semiconductor crystal is smaller than the exciton Bohr radius, the band gap can be also engineered by controlling the size of the nanocrystal. In such small sizes of around 10 nanometers, the wave functions of electron and hole are spatially confined. This effect is called quantum confinement and the nanocrystals in the range of this regime are called quantum dots (QDs).

The theoretical relation between the size of the quantum dots and the energy gap was first described by a model under the assumption of a spherically symmetric potential well of infinite depth [1]. According to the model, the energy gap is inversely proportional to the square of the radius of the quantum dot. This means that as the size

of the quantum dot decreases, the energy gap exponentially increases which corresponds to a blueshift in the emission and absorption color of the quantum dot and vice versa. The representation of the relation between the physical size of the quantum dots and the optical features of them can be seen in Figure. 1.1.1.

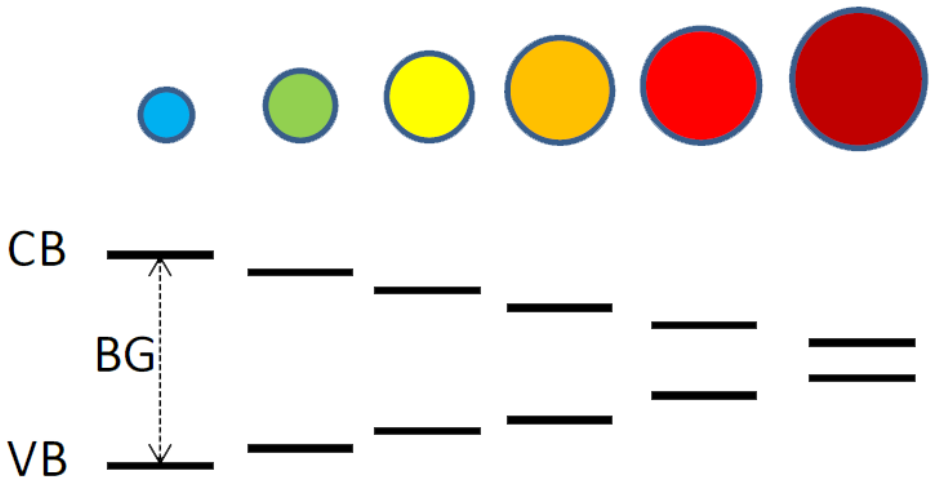


Figure. 1.1.1 Optical features (band gaps) of the quantum dots according to their sizes. Here, the CB refers to conduction band minimum while VB stands for the valence band minimum. As the size of the nanocrystal increases, the energy bandgap (BG) between CB and VB decreases.

The discrete energy levels caused by quantum confinement of the quantum dots make atomic-like pure emissions possible. With the advancements in the colloidal synthesis techniques and the understandings of the structural compositions of the materials, the emission efficiencies of quantum dots dramatically increased to 50% in 15 years [4]. This improvement was an important milestone towards today's quantum dots with near-unity (100%) photoluminescence quantum yield [5,6].

Thanks to advantageous optoelectronic properties of quantum dots such as size-dependent tunable emission color, narrow band emission, high quantum yield, high stability and solution processability; they received a great amount of research interest [7,8]. For a long time, CdSe based QDs have focused the research efforts on them. However, with the increasing concerns about the environment, the toxicity of Cd led the research focus on the synthesis of high-quality quantum dots to new materials such as InP based ones [9,10].

## 1.2 Introduction to Perovskite Nanocrystals

Most recently, a new colloidally synthesized nanoparticle form of an already known material namely lead halide perovskites was presented [11,12]. While the other type of quantum dots needed decades-long investigations to reach high-quality levels, the perovskite quantum dots were reported with as high as 90% photoluminescence quantum yield (PLQY) and narrower emission linewidth (12 - 42 nm) values since their early days. Additionally, the facile and low-cost colloidal synthesis of the perovskite quantum dots and the ability of perovskite quantum dots to cover the whole visible spectrum by easily tuning the emission wavelength either with the nanocrystal size or the halide composition encouraged many researchers to focus his/her efforts on this new nanocrystal.

The chemical formula of all-inorganic lead halide perovskites is $CsPbX_3$, where the X can be Cl, Br, I or the composition of them. The crystal structure of the CsPbBr3 perovskite quantum dot can be seen in Figure. 1.2.1. While in this thesis, this type of perovskites are on the focus, there are other possible compositions of perovskite structures in the literature, for example: organometallic halide perovskites which replaces Cs with the organic molecules such as $CH_3NH_3$ = methylammonium (MA) or $CH(NH_2)_2$ = formamidinium (FA) [11,13], and hybrid organic-inorganic perovskites of $Cs_{1-x}FA_xPbX_3$ [14], and doped perovskites such as $CsPbCl_3$:Mn [15], and Pb free perovskites such as $Cs_2SnI_6$ or $Cs_3Cu_2Br_{5-x}I_x$ [16][17].

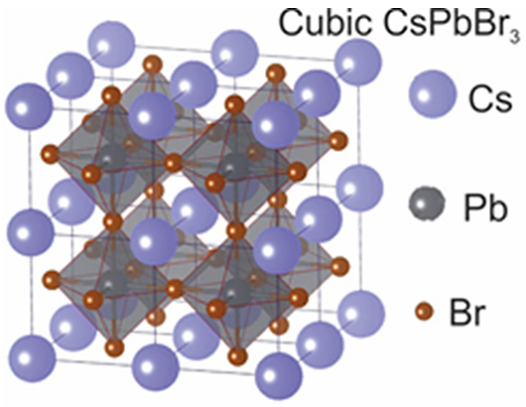


Figure. 1.2.1 The crystal structure of the CsPbBr3 perovskite quantum dot. The image was adapted from reference [12]

The best and easiest way of color tuning for colloidal perovskite quantum dots is to change the composition of the halide component unlike other types of quantum dots. To cover the all visible range of spectrum Cl is used for blue and Br is used for green, for the tones between them the mixture of Cl and Br is used, while I is used for red, the mixture of Br and I is used for the color tones between green and red. The photographs of the full-color spectrum colloidal perovskite quantum dots under daylight (a) and under ultraviolet light (b), and the graph shows the photoluminescence emissions (c) and the absorbance spectrums (e) can be seen in Figure. 1.2.2. One of the incredible features of perovskite quantum dots is that it is possible to tune the emission wavelength of them even after the synthesis. This process is called anion exchange [18]. It is such a process which can be done at room temperature and in a few seconds. It is as easy as to mix two solutions: one is the colloidal perovskite quantum dot solution and the other is the anion exchange precursor solution.

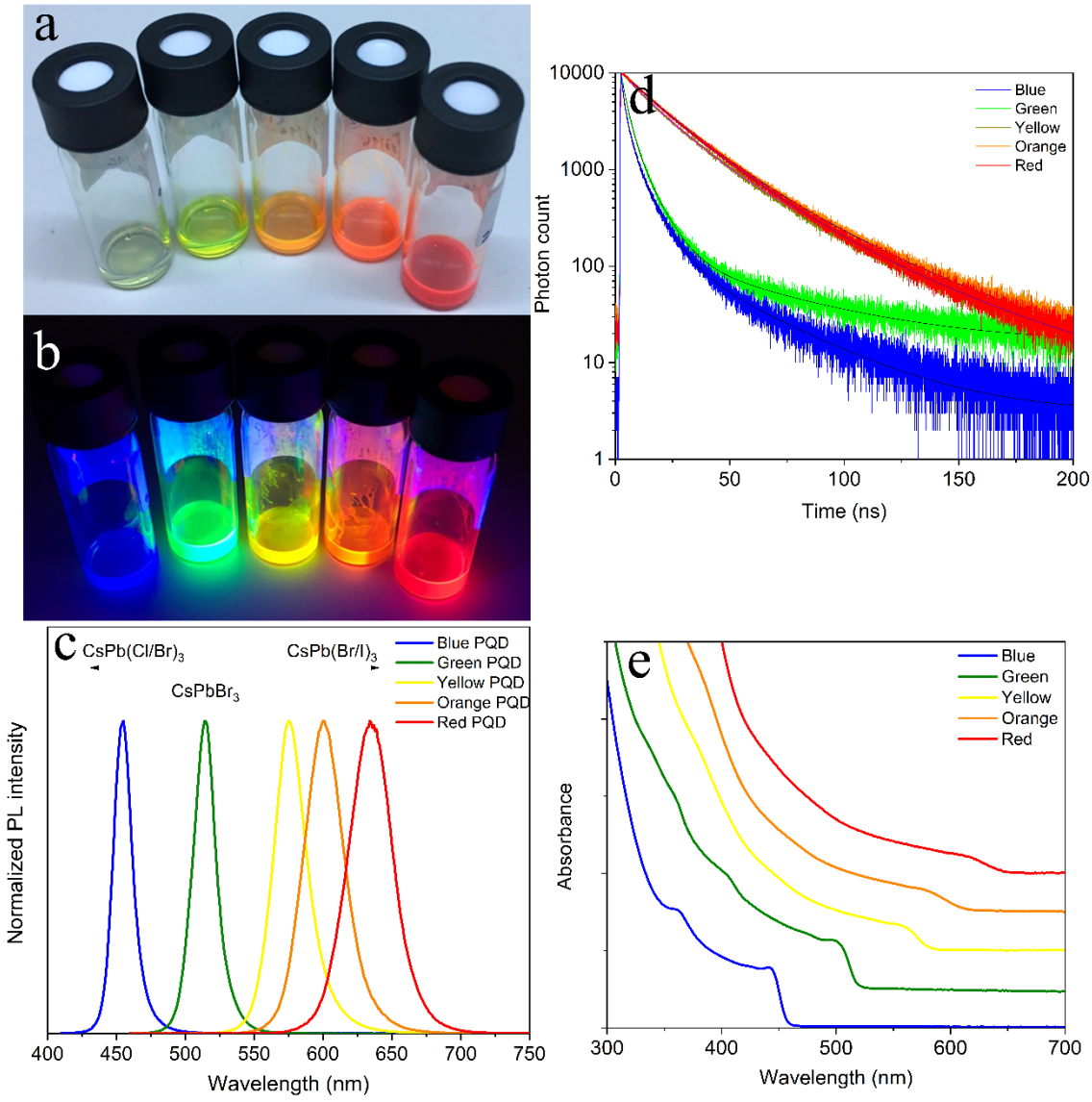

Figure. 1.2.2 Colloidal perovskite quantum dots covering the whole visible spectrum. The photographs of them under daylight (a), and under UV light (b). The spectra of their photoluminescence emissions (c), and absorbances (e). The time-resolved photoluminescence decays of the perovskite quantum dots (d). The figure was adapted from the reference [19]

The unique optoelectronic and chemical properties of colloidal quantum dots such as high efficiency, narrow linewidth, color tunability, solution processability, ligand changeability, polymer compatibility made them promising materials for future applications such as display technologies [20–23], light-emitting diode (LED) technologies [24–30], bio labeling and imaging technologies [31], photovoltaic technologies [32,33] and lasing technologies [34].

## 1.3 Introduction to Light Emitting Diode Applications of Nanocrystals (QLEDs)

The perfect optoelectronic features of the colloidal quantum dots encouraged the commercial efforts to be especially on the down-conversion applications in the TV and lighting industry. The LCD displays have a white back-lighting actually based on blue LEDs. The white light is generated with the yellow phosphors coated on the LED chips. The very same chips are also used in lighting. However, the white light generated by this way is very low quality in terms of either standarts of National Television System Committee (NTSC) and Color Rendering Index (CRI). The color gamut coverage of the NTSC, for the LCD televisions which use conventional yellow phosphor down-converters is only 72% [35]. It is such a low value because the white light is generated by only two color and the yellow is extremely broad. In order to create a high-quality light at least three colors of blue, green and red with pure emissions (narrow full-width half-maximum) are needed. By replacing the conventional phosphor, it is possible to generate a high-grade white (R+G+B) light with the color gamut coverage of the NTSC: 122.5%, and CRI as high as 88.6 with the 290 $lm/W_{op}$ luminous efficacy and having a warm white shade at a correlated color temperature of 2763 K.[22].

The ace players of the global display producer companies such as Samsung, Hisense, TCL invested in quantum dots technology and are working with the start-up companies such as Najing Tech, QD vision and Nanosys. The TV companies are producing QLED televisions and they are increasing the production capacities year by year. Recently, Samsung announced that they will invest $11 billion in quantum dot display manufacturing to increase the capacity [36].

The next and the ultimate step for the display industry would be to use the exciting technology of quantum dots as electroluminescents. In contrast to photoluminescence, electroluminescence (EL) does not need a higher energy light to generate photons, nevertheless, it requires electrical current. In electroluminescence, charges of electron and holes are injected into the quantum dots to generate excitons (electron – hole pair) which generate photons during recombination. The electroluminescent devices which use quantum dots as emissive layer are called Quantum Dot Light Emitting Diodes (QLEDs). Since the QLEDs offer a combination of perfect optoelectronic and physical properties such as high device efficiency, high color purity, lightness, and flexibility, they were seen as a serious candidate for next-generation display and lighting technology. For this reason, for more than two decades, QLEDs are the focus of intense research towards commercialization [24–30]. In this time period, the External Quantum Efficiency (EQE) performances of QLEDs reached nearly the theoretical limits. For the Cd based ones Dai X. et al reported 20.5% EQE for red QLED [26], Acharya K. P. et al. reported 21% EQE for green QLED [37], and Wang L. et al. reported 19.5% EQE for blue QLED [38]. For the all-inorganic lead halide perovskite quantum dots based Light Emitting Diodes, Li J. et al. reported 6.27% EQE for $CsPbBr_3$ (green) QLED [29], and Chiba T. et al. reported 21.3% EQE for $CsPb(Br/I)_3$ (red) QLED [30].

# Chapter 2

# Light Emitting Devices Based On Nanocrystals and Their Working Principles

The light-emitting diode applications of the nanocrystals can be considered under the two main subgroups (Figure. 2.1). The first one is the applications in which the nanocrystals are used as the photoluminescent layers (PL), and the second one is the applications in which the nanocrystals are used as the electroluminescent layers (EL). In the photoluminescent applications of the nanocrystals, the light is created by another LED. The PL layers are placed on top of the LED. Generally, the color of the LED is blue and the colors of the nanocrystals in the PL layers are green and red. With this simple method, a very high-quality white light can be generated for the displays or the illumination. The efficiency of the light is directly related to quantum yield (QY) of the nanocrystal. However, in the electroluminescent applications of the nanocrystals, the light is created by the nanocrystals itself. The electric current is converted into light. This type of light-emitting diodes require more sophisticated fabrication methods. The efficiency of the light is not only related to QY of the nanocrystal but also the structure and the fabrication methods of the LED.

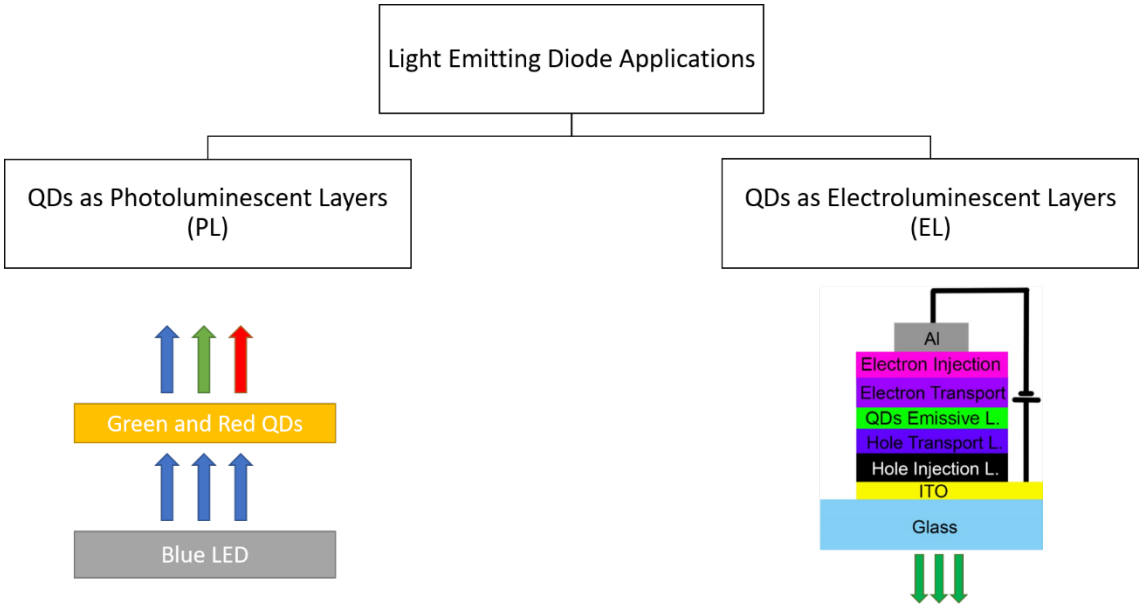


Figure. 2.1 The light-emitting diode applications of the nanocrystals

The device structure of QLEDs is composed of stacked thin films. The arrangement of the layers is as transparent anode / hole injection layer (HIL) / hole transport layer (HTL) / quantum dots layer or emissive layer (EML) / electron transport layer (ETL) / electron injection layer (EIL) / Cathode. The typical device structure of a QLED can be seen in Figure. 2.2. The injection layers inject charge carriers to the transport layers and they transport charge carriers to the QDs layer. The transported electrons and holes form excitons and generate photons by radiative recombinations. The energy of the generated photon corresponds to the bandgap of the quantum dot.

In order to generate the maximum light from a QLED, the choice of the materials of the charge transport layers must be made appropriately. The highest occupied molecular orbital (HOMO) and the lowest unoccupied molecular orbital (LUMO) positions of the charge transport layers relative to nanocrystals and the charge mobility of the charge transport layers are very important parameters for an efficient and balanced charge injection. Last but not least, the quantum efficiency of the nanocrystal layer directly affects the efficiency of the light-emitting diode. For the best results, the colloidal nanocrystals with the highest quantum yield must be used. However, it is not sufficient the nanocrystals to have a high quantum yield at the only colloidal state, they must have high quantum yield at the thin film state too. Generally, the shell thickness and the density of the ligand of the nanocrystals are the determining factors of quantum yield at the thin-film state.

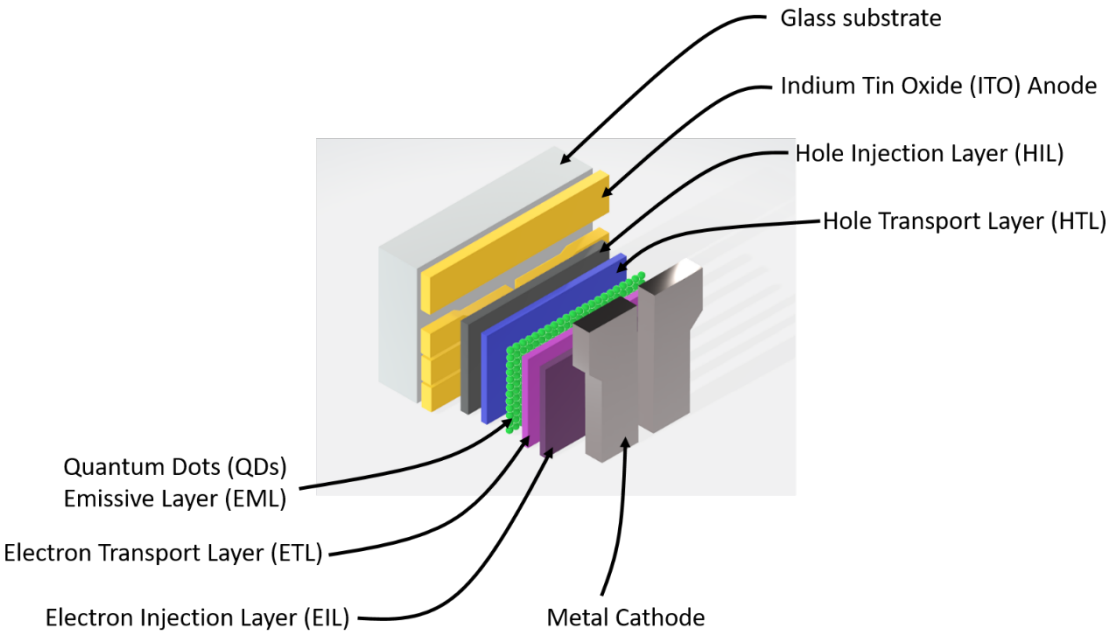


Figure. 2.2 The layer structure of a QLED device

The fabrication of a light-emitting diode device has been performed for the first time in the Abdullah Gül University within the scope of this thesis. Therefore, the whole thesis should be considered as an optimization study for the inception of the fabrication and the characterization of the nanocrystals based light-emitting diodes. So, the initial optimization studies of the light-emitting diodes were performed on the relatively stable, classical semiconductor-based nanocrystals such as CdSe/ZnS quantum dots. In this regard, semiconductor nanocrystals based blue and green light-emitting diodes were fabricated. As a proof of concept, flexible blue LEDs based on semiconductor nanocrystals were fabricated. Then, a photoluminescent layer consisting of red and green semiconductor nanocrystals were placed on the flexible blue LED to generate white light. After that, the perovskite nanocrystals based light-emitting diode fabrication was optimized.

## 2.1 Proof of Concept: Cd Based Flexible White LED

High efficient, cost effective, flexible and high quality white light emitting sources are essential for future lighting and display technologies. Not only with the high quality features but with the chemical properties such as solution processability, the colloidal quantum dots are the most promising candidates for flexible, bendable, stretchable and deformable new generation, high quality white light emitting diodes.

The increasing use of smart devices and growing demand for mobility requires lighter weight, more efficient, flexible and feasible components. Similarly, increasing environmental concerns require high efficient light sources. As a next generation light source, quantum dot light emitting diodes (QLEDs) have a great potential and attracted considerable amount of interest since 1994 [24]. Great efforts have been made to increase performance and mobility of the QLED devices but most of them were focused on single colored QLEDs [26,39–44]. Only a minority of these research efforts were for white QLEDs (WQLEDs) [45–51]. Most of the WQLED studies offer methods such as mixing R, G, B QDs in emissive layer, quantum dots (QD)-based down-conversion and recently reported tandem QLED structures. However, all these methods have disadvantages along with their advantages. For example, using mixed QDs in emissive layer leads to luminescence quenching and self-absorption issues and extremely sensitive dependency to color component proportions and solution concentration makes it almost impossible to reproduce same quality of white light [52]. Although QD-based down-conversion method meets commercialization requirements, since the InGaN LED chip is used as excitation source, the method lacks flexibility, large area emission and low cost fabrication. As a relatively new and promising method, the tandem structured WQLEDs, despite their high efficiency, have a complex architecture and increased difficulty of building the device flawlessly.

In this proof of concept study, it was brought together the ease and efficiency of monochromatic QLEDs and the commercial promise of QD-based down conversion technique. A flexible white QLED with the CRI of up to 90.5 and the CCT of 3239K of high quality white light. The flexible design consists of blue emitting CdZnS/ZnS nanocrystals based QLED fabricated on ITO coated PET substrate and an InP based

green and red QDs containing flexible polymer film as down-converting component and epoxy as adhesive. The Förster resonance energy transfer (FRET) between green and red QDs was also demonstrated in the polymer film. Additionally, the CRI and CCT difference between WQLEDs was showed when FRET is present and absent.

Although the method relies on the great knowledge in the literature, the current state of the art of blue QLEDs is not suitable for commercialization yet [53]. When the necessary improvements are made for the blue QLEDs, the offered relatively easy method for generating white light from QDs and flexible structures would be a promising candidate for next generation lighting and displays.

### 2.1.1 Results and Discussion

Normalized photoluminescence characteristics of the synthesized highly luminescent QDs can be seen in Figure. 2.1.1.1 together. The blue-emitting CdZnS/ZnS QDs were synthesized with a peak photoluminescence emission wavelength of 445 nm, a quantum yield of 96% and a full-width at half-maximum (FWHM) of 23 nm. The blue-emitting QDs were used as emissive layer in the device structure of flexible QLED. The green-emitting InPZnS/ZnS QDs were synthesized with a peak PL emission wavelength of 510 nm, a quantum yield of 56% and a FWHM of 51 nm. The red-emitting InP/ZnS QDs were synthesized with a peak PL emission wavelength of 614 nm, a quantum yield of 50% and a fwhm of 58 nm. The green-emitting and red-emitting QDs were used as color converters in a flexible polymer film matrix adherent on top of the flexible QLED for white light generation.

Figure. 2.1.1.2 a) shows current-voltage curve of the blue QLED. The images of the flexible and non-flexible blue emitting QLED devices and, the flexible white LED can be seen in Figure. 2.1.1.2 b), c) and d), respectively. The structure of the device as follows: Poly(2,3-dihydrothieno-1,4-dioxin)-poly(styrenesulfonate) (PEDOT:PSS) / Poly(9-vinylcarbazole) (PVK) / CdZnS/ZnS QDs / ZnO nano particles / Aluminium.

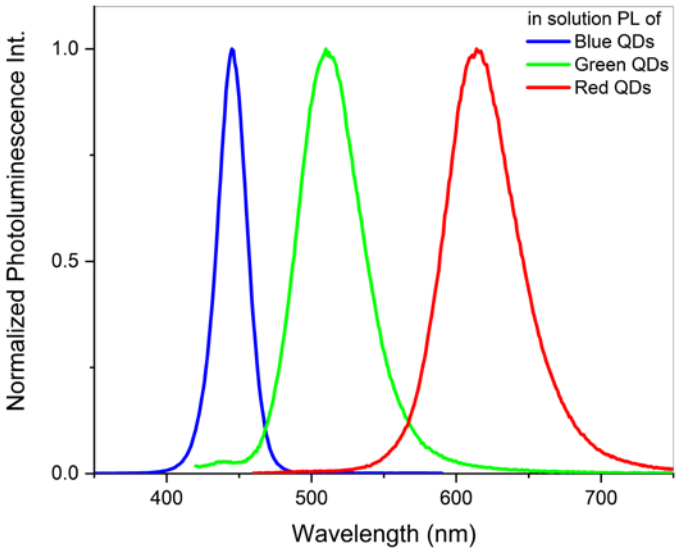


Figure. 2.1.1.1 Normalized photoluminescence graphics of blue-, green- and red-emitting quantum dots in solution

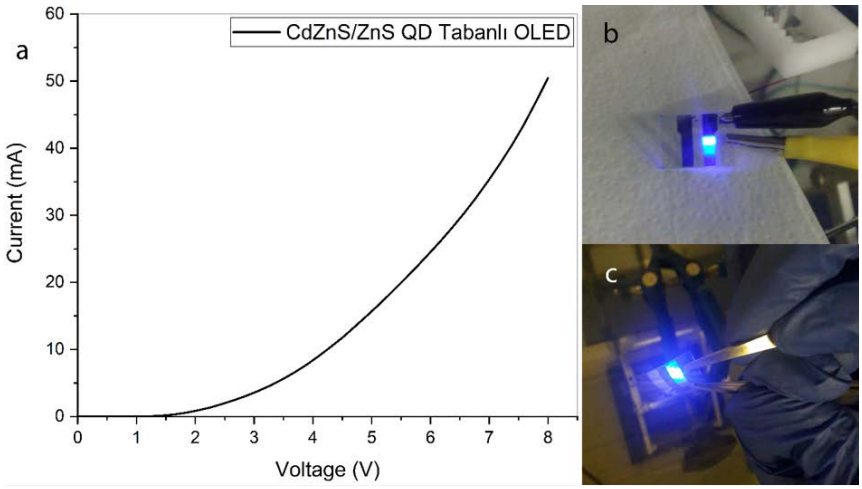


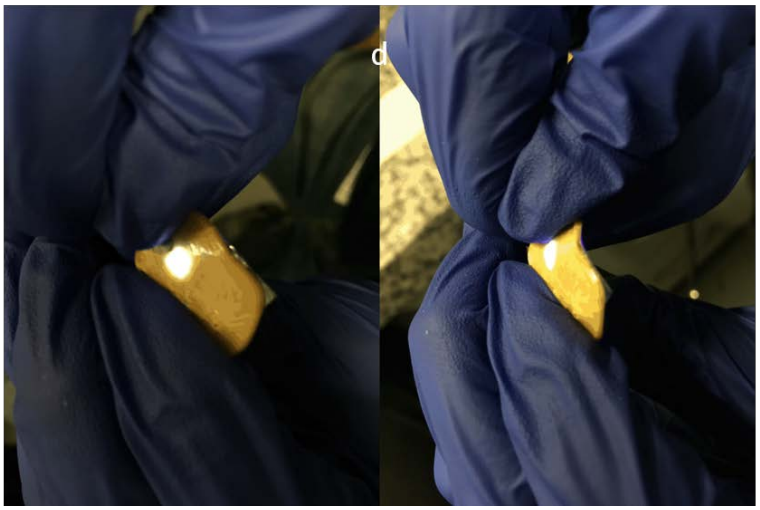


Figure. 2.1.1.2 a)Current-voltage curve of the QLED, images of blue emitting b)non-flexible, c) flexible QLEDs, d) flexible white LED

The color rendering index (CRI) of up to 90.5 and correlated color temperature (CCT) of 3239 K was achieved with a flexible color converter film on a flexible blue QLED. This film contained a blend of green and red QDs. With this configuration of green and red QDs in flexible polymer film, we showed and analysed a nonradiative energy transfer between green and red QDs. We also prepared two other films. One contained only equal amount of green QDs and the other contained only equal amount of red QDs as in the blended film. We investigated the energy transfer by comparing these two films with the blended film. We made time-correlated single photon counting measurements and photoluminescence spectrum measurements. Additionally, we calculated the CRI and CCT values for unblended films by putting them top of each other on the blue QLED. Figure. 2.1.1.3 a) shows the spectral difference of white light generated by blended film and unblended films top of each other on flexible blue QLED. The CRI and CCT values calculated for unblended films on flexible QLED turn out to be 82.6 and 6422 K, respectively. In the figure, the Förster resonance energy transfer can be seen clearly. Although the films contain same amount of QDs, the fluorescence intensity of green QDs in unblended film is higher than the green QDs in blended film. However, the fluorescence intensity of red QDs in unblended film is lower than the red QDs in blended film. The time-correlated single photon counting decays of the QDs in different films can be seen in Figure. 2.1.1.3 b) The lifetime analysis results of these decays are given in Table 2.1.1.1. According to these results and decays the lifetime of the donor green QDs decreases from 63.78 ns to 51.94 ns and the lifetime of the acceptor red QDs increases from 27.29 ns to 64.55 ns when they are blended in the same film.

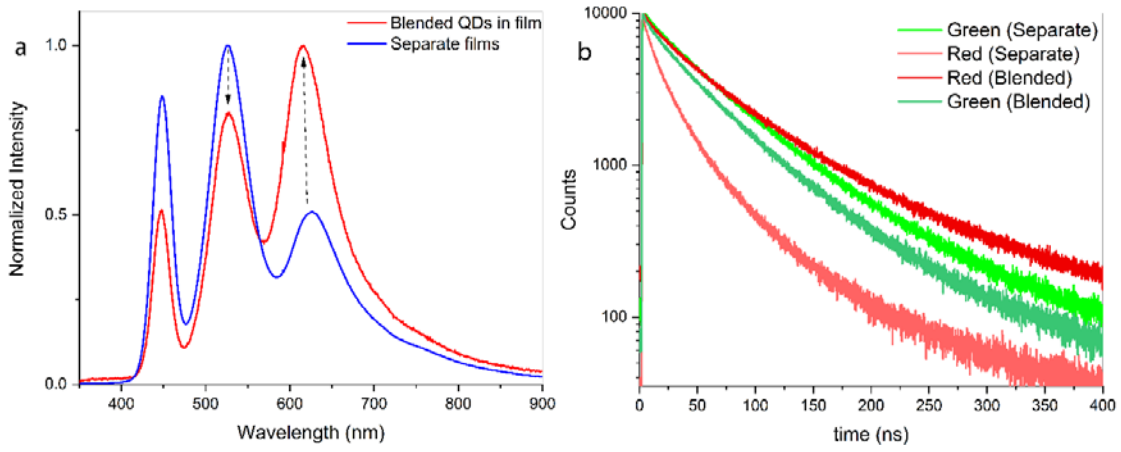

Figure. 2.1.1.3 a) The spectrum difference of white lights generated by blended red and green QDs in a film and separate red and green films, b) the time-correlated single photon counting decays of the blended QDs in a film and separate films of QDs

| Sample | $A_1$ | $\tau_1$(ns) | $A_2$ | $\tau_2$(ns) | $t_{ort}$(ns)(ampl.) |
|---|---|---|---|---|---|
| Green (Separate) | 4140.8 ±27.3 | 84.5 ±0.4 | 3744.4 ±51.0 | 40.9 ±0.6 | 63.78 |
| Red (Separate) | 2105.5 ±29.0 | 59.9 ±0.6 | 6386.1 ±96.8 | 16.6 ±0.3 | 27.29 |
| Red (Blended) | 5662.8 ±30.4 | 87.5 ±0.4 | 3658.9 ±72.5 | 28.9 ±0.6 | 64.55 |
| Green (Blended) | 5213.8 ±34.0 | 70.3 ±0.3 | 3960.6 ±73.8 | 27.8 ±0.5 | 51.94 |

Table 2.1.1.1 The analysis results of the lifetime decays

# 2.2 Cadmium Based Blue Emitting LEDs

A hero device with a 16 % external quantum efficiency (EQE) was fabricated with blue emitting cadmium based quantum dots. The luminance of the device is near 3000 cd/m$^2$ and turn-on voltage is 6 V. The emission wavelength is close to 450 nm. As it can be seen from the Figure. 2.2.1, the device has a stable performance above the 1 % of EQE until very high voltages. It is the most efficient QLED fabricated in our research group's lab (collaborative work with PhD student Kaan Elmacıoğlu and Dr. Yemliha Altıntas) and is very close to literature records. The structure of the device as follows: Poly(2,3-dihydrothieno-1,4-dioxin)-poly(styrenesulfonate) (PEDOT:PSS) / Poly(9-vinylcarbazole) (PVK) / CdZnS/ZnS QDs / ZnO nano particles / Aluminium. In this regard, this structure is very promising for catching the records in the near future for our group.

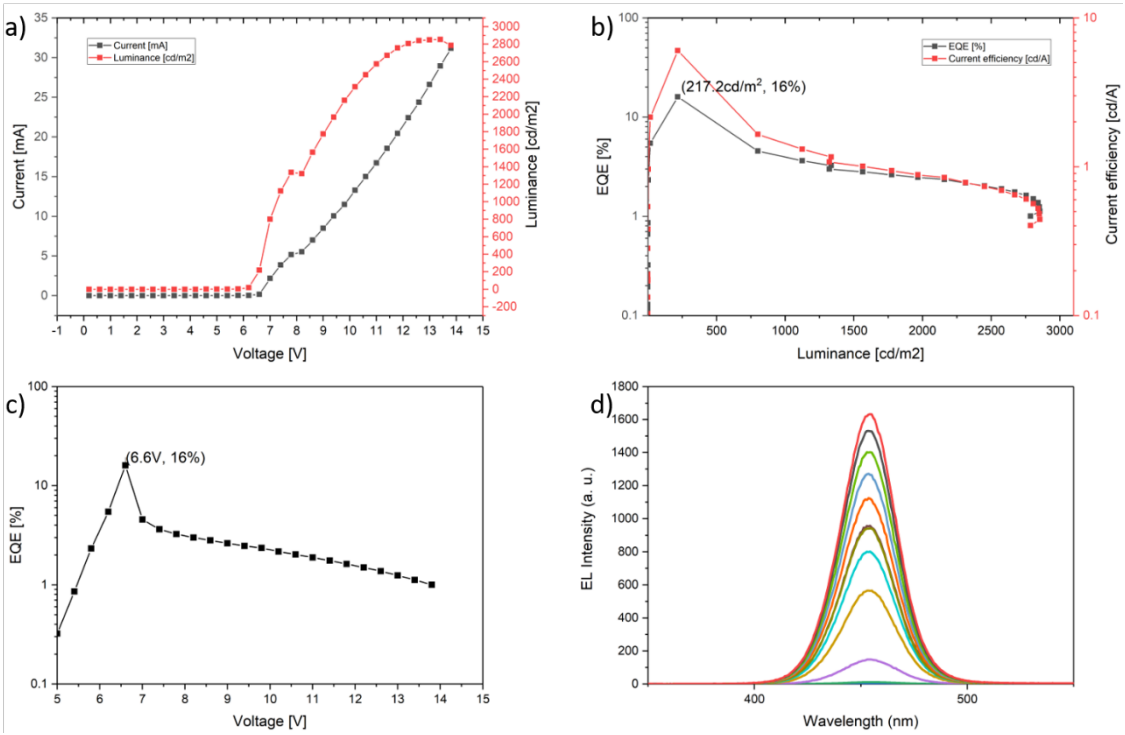


Figure. 2.2.1 The characterization results of the most heroic device of our research group, cadmium based blue light emitting diode. a) voltage vs. current and voltage vs. luminance, b) luminance vs. external quantum efficiency (EQE) and luminance vs. current efficiency, c) voltage vs. EQE, d) emission spectra of the LED at different voltages

## 2.3 Cadmium Based Green Emitting LEDs

A very bright, green emitting Cd based QLED with nearly 40,000 cd/m$^2$ luminance was fabricated. It has 3.2 % external quantum efficiency (EQE) and a stable profile at high voltages. The results of the device can be seen in Figure. 2.3.1. The structure of the device as follows: Poly(2,3-dihydrothieno-1,4-dioxin)-poly(styrenesulfonate) (PEDOT:PSS) / Poly(9-vinylcarbazole) (PVK) / CdZnS/ZnS QDs / ZnO nano particles / Aluminium.

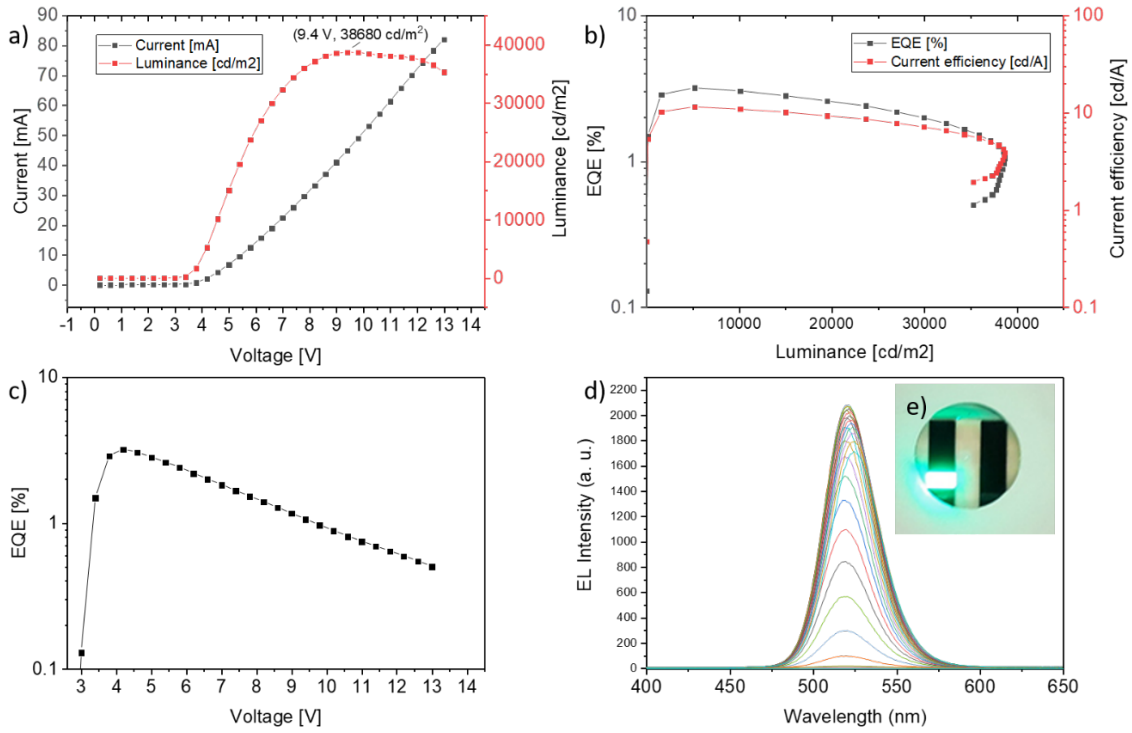


Figure. 2.3.1 The characterization results of cadmium based green light emitting diode. a) voltage vs. current and voltage vs. luminance, b) luminance vs. external quantum efficiency (EQE) and luminance vs. current efficiency, c) voltage vs. EQE, d) emission spectra of the LED at different voltages, e) the photograph of the LED

## 2.4 All-Inorganic Perovskite Nanocrystals and LED Applications in the Literature

Recently, Li J. et al. [29] reported a green emitting perovskite light emitting diode with a maximum EQE value of 6.27% (Figure. 2.4.1). The device structure is Poly(2,3-dihydrothieno-1,4-dioxin)-poly(styrenesulfonate) (PEDOT:PSS) / Poly(N,N'-bis-4-butylphenyl-N,N'-bisphenyl)benzidine (Poly-TPD) / perovskite nanocrystals / 2,2',2''-(1,3,5-Benzinetriyl)-tris(1-phenyl-1-H-benzimidazole) (TPBi) / lithium fluoride (LiF) / aluminium (Al). They used a controlled purification method with hexane / ethyl acetate mixture to precisely control the surface ligand density of the colloidal perovskite nanocrystals. The best result is achieved with a purification of two times.

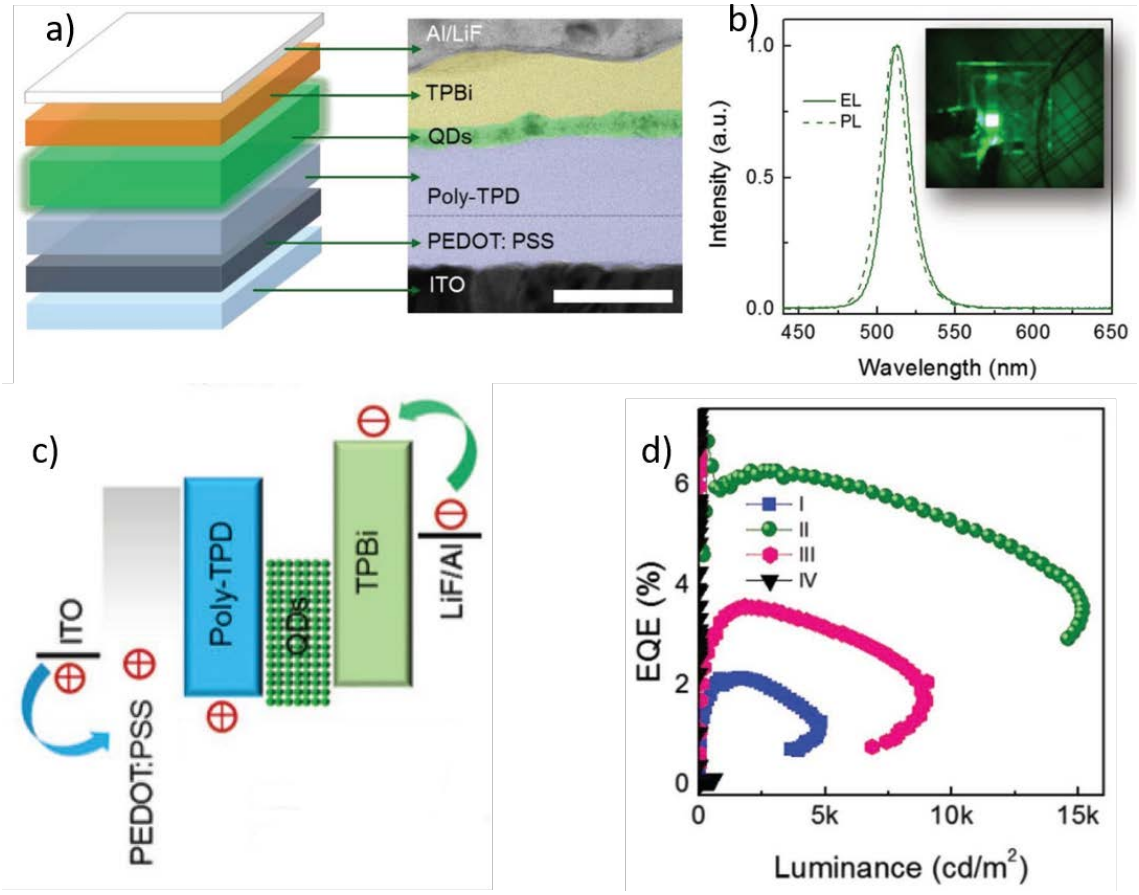


Figure. 2.4.1 The specifications of the perovskite nanocrystal based light emitting diodes in the reference (figures were adapted from the reference) [29]: a) device structure, b) emission spectra of the QD and the LED, c) band structure in the device, d) external quantum efficiency (EQE) vs. luminance measurement results of the LED devices based on perovskite nanocrystals purified I, II, III and IV times

Most recently, T. Chiba et al. [30] reported a red emitting perovskite light emitting diode with a maximum EQE value of 21.3% in the literature (Figure. 2.4.2). The device structure is Poly(2,3-dihydrothieno-1,4-dioxin)-poly(styrenesulfonate) (PEDOT:PSS) / Poly(N,N'-bis-4-butylphenyl-N,N'-bisphenyl)benzidine (Poly-TPD) / perovskite nanocrystals / 2,2',2''-(1,3,5-Benzinetriyl)-tris(1-phenyl-1-H-benzimidazole) (TPBi) / lithium fluoride (LiF) / aluminium (Al). They fabricated the quantum dots by anion exchange from pristine $CsPbBr_3$ using halide-anion-containing alkyl ammonium and aryl ammonium salts. During the anion exchange, at the same time, the ligands were also changed. This record high value of EQE was attributed to the perfectly suitable new ligands.

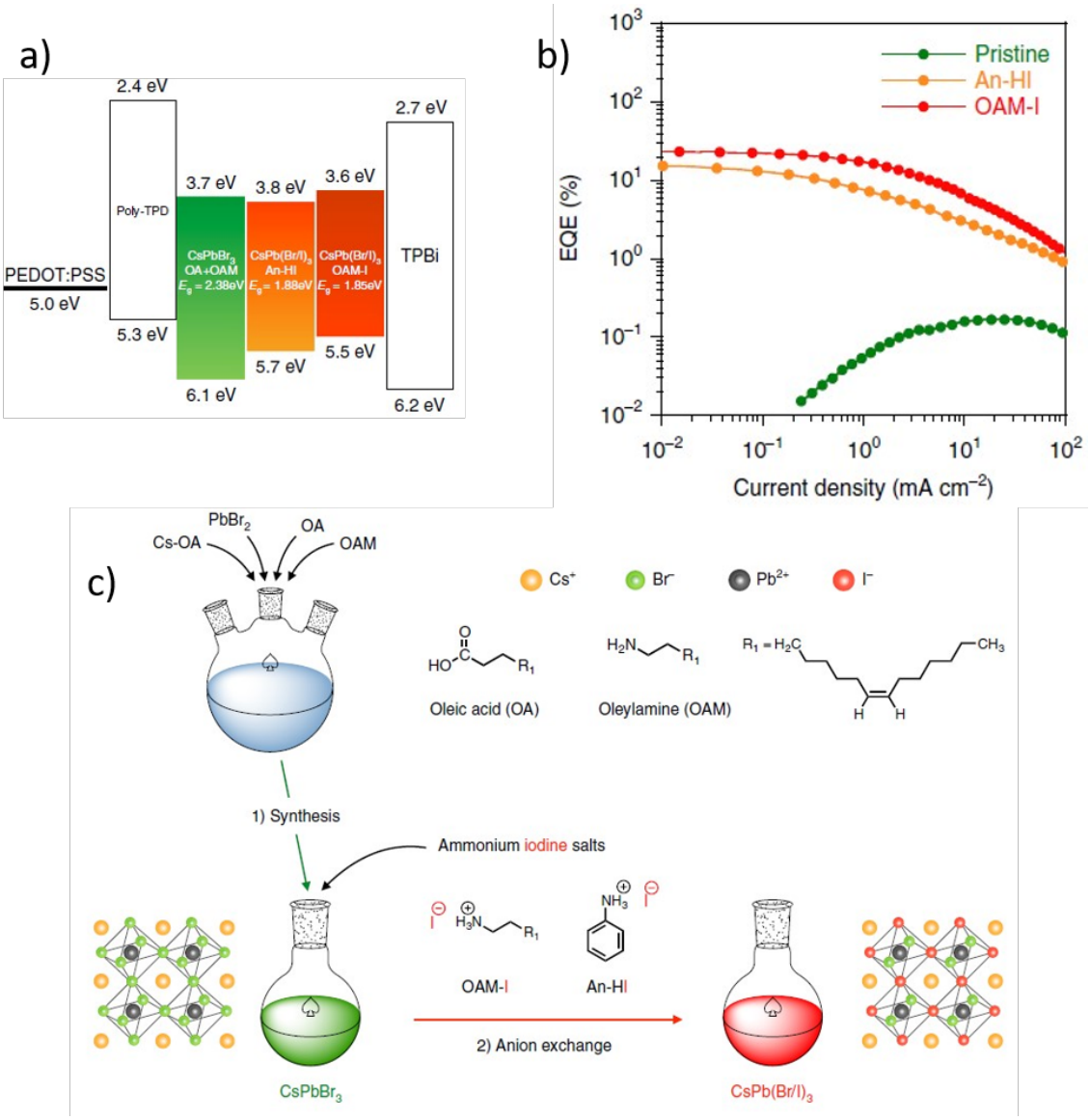


Figure. 2.4.2 The specifications of the perovskite nanocrystal based light emitting diodes in the reference (figures were adapted from the reference) [30]: a) band structure in the device, b) external quantum efficiency (EQE) vs. current density measurement results of the LED devices based on perovskite nanocrystals with different ligands and anions

# Chapter 3

# Experimental Methods

## 3.1 Synthesis of Colloidal Perovskite Nanocrystals

Perovskite QDs have been synthesized and purified according to ref. [12], [54] and [55] with slight modifications as described below.

### 3.1.1 Preparation of Cs-oleate Precursor

0.407 g of $Cs_2CO_3$, 20 mL of octadecene (ODE) and 1.55 mL of oleic acid (OA) were loaded into a 50 mL flask and dried under vacuum for 1h at 120 °C. Then mixture was heated to 150 °C under argon. After the complete dissolution the solution became transparent and ready to be used. The remaining precursor solution is stored in glove box and heated to 150 °C before use.

### 3.1.2 Synthesis of $CsPb(Br/I)_3$ Red Perovskite QDs

0.0625 mmol of $PbBr_2$, 0.125 mmol of $PbI_2$ and 5 mL of ODE were loaded into a 25 mL flask and dried under vacuum for 1 h at 120 °C. Then 0.5 mL dried oleylamine (OLA) and 0.5 mL dried oleic acid (OA) were injected to flask at 120 °C under Ar flow. After the dissolution of the mixture the flask was heated to 160 °C. After 15 min. preheated 0.4 mL of Cs-oleate solution was swiftly injected into the flask and 5s later, the mixture was cooled down by an ethanol bath.

### 3.1.3 Synthesis of $CsPbBr_3$ Green Perovskite QDs

The green-emitting perovskite nanocrystal quantum dots were synthesized following a very similar procedure. The only differences are that flask is loaded only with 0.187 mmol of PbBr2 and the final temperature is set to 180 °C.

### 3.1.4 The Purification of Perovskite Quantum Dots

The synthesis was taken to the 50 mL falcon tube and centrifuged for 3 min at 5000 rpm. The supernatant was discarded. The precipitate was dispersed in 300 µL hexane or octane. The solution was centrifuged again at same speed and duration. This time precipitate was discarded. Again 300 µL hexane or octane was added to supernatant and solution was mixed. Then 600 µL ethyl acetate was added and the solution centrifuged again at same settings. The supernatant was discarded and precipitate was dispersed in 600 µL hexane or octane. (From the beginning, the same solvent should be used.) The density of the QDs solution is adjusted prior to use for QLED fabrication.

## 3.2 Device Fabrication of Perovskite Light Emitting Diodes

Perovskite quantum dot light emitting diodes were fabricated on to patterned ITO substrates with a device structure of ITO/Pedot:PSS/Poly-TPD/QDs/TPBi/LiF/Al. The substrates were cleaned with Hellmanex III and deionized water in sonicator for 15 min and the substrates were washed with deionized water two times in sonication bath. Lastly, the substrates were sonicated with isopropanol for 15 min. Then the substrates were dried with nitrogen gas flow. The cleaned substrates were then placed into an oxygen plasma device for 20 min. At the same time, Pedot:PSS was sonicated for 10 min and filtered. The substrates were spin-coated by Pedot:PSS at the speed of 2000 rpm for 1 min and were annealed at 150 °C for 20 min. Next, the substrates were placed in a glove box and all the next steps were performed under inert conditions. In the glove box, poly-TPD in chlorobenzene (10 mg/ml) was spin-coated at 4000 rpm with a 2000 rpm of ramp for 1 min and the substrates were annealed at 120 °C for 15 min. The QDs in dried octane (10 mg/mL) (or hexane) was spin-coated at 4000 rpm with a 2000 ramp for 1 min and the substrates were annealed at 60 °C for 15 min. Then, the substrates were placed in a thermal evaporator within an active area mask and the organic electron transport material of TPBi of 20 nm was deposited under high vacuum. Then the substrates were moved to a cathode mask. The LiF of 1 nm and Al of 100 nm was deposited under high vacuum. Lastly, the QLEDs were encapsulated by an epoxy and glass layer.

## 3.3 Synthesis of Cd based QDs

### 3.3.1 Synthesis of Blue-Emitting CdZnS/ZnS QDs

The CdZnS/ZnS QDs were prepared following a modified literature procedure [56]. 1 mmol of CdO, 10 mmol of Zinc acetate and 7 mL of OA were mixed in a 3-neck

flask. The mixture's temperature was increased to 100 °C under vacuum for an hour and then heated to 150 °C under Ar. Then, 15 mL of ODE was added into flask and the mixture was heated to 310 °C. Then, a sulphur (S) stock solution of 1.6 mmol of S dissolved in 2.4 mL of ODE was swiftly injected into flask. After 12 min of CdZnS core growth, a S stock solution of 4 mmol of S dissolved in 5 mL of OA was added dropwisely at a rate of 0.5 mL/min, for the ZnS shell coating. After 3h of shell growth, the mixture was cooled in a water bath. The resulting QDs were precipitated by adding excess ethanol, centrifuging and then dispersed in hexane.

### 3.3.2 Synthesis of Green-Emitting CdSe/ZnS QDs

The synthesis of green emitting CdSe/ZnS QDs was carried out according to a modified method in the previous literature [22], [57,58]. 0.3 mmol of CdO and 4 mmol of zinc acetate (ZnAc) were loaded with 5 ml of oleic acid in a 50 mL three neck flask and dried under vacuum at 150 °C for 30 min. Then, the solution was cooled down to 50 °C and 15 mL of 1-ODE was loaded in to the flask and heated to 100 °C under vacuum. After the Ar gas flow, the temperature was rised to 300 °C to obtain the transparent mixed solution of cadmium oleate and zinc oleate. Separately, a mixture of 0.3 mmol of Se and 3 mmol of S were dissolved in 2 mL of TOP at room temperature in the glove box. The clear solution of Se and S in TOP was swiftly injected into the reaction flask at 300 °C and the solution was kept for 10 min more. Then, the mixture was cooled down to room temperature. The synthesized QDs are transferred to the falcon tubes. A precipitation and re-dispersion method was used for the cleaning of QDs. The crude solution was precipitated in the presence of absolute acetone and methanol by centrifugation at 5000 rpm for 15 min and finally QDs have been re-dispersed in the hexane.

## 3.4 Synthesis of ZnO Nanoparticles

The ZnO nanoparticles were synthesized according to a modified literature method. 3 mmol of Zinc acetate dihydrate was dissolved in 30 mL DMSO. 5 mmol of tetramethylammonium hydroxide pentahydrate (TMAH) was dissolved in 10 mL of ethanol under inert atmosphere in glove box. The TMAH solution was added to zinc acetate dihydrate solution under stirring with a rate of 7 mL per min under atmosphere. After 1 h of mixing the solution was divided into three tubes having equal volume. The empty space of falcons were filled with acetone and centrifuged at 5000 rpm for 5 min. The supernatant was discarded and precipitates were dispersed in 1 mL of ethanol. Then each falcon tube was loaded with 24 mL of acetone and 25 mL of hexane. The tubes were centrifuged for 10 min at 5000 rpm. The precipitates were dispersed in ethanol by the cold sonication bath. After the dissolution, they were filtered with a 0.45 um filter. Their density were adjusted to 30 mg per mL and stored in freezer.

## 3.5 Device Fabrication of Blue and Green Emitting Cd Based QLEDs

Flexible quantum dot light emitting diodes were fabricated on to patterned ITO PET substrates with a device structure of indium tin oxide (ITO) / Poly(2,3-dihydrothieno-1,4-dioxin)-poly(styrenesulfonate) (PEDOT:PSS) / Poly(9-vinylcarbazole) (PVK) / QDs / ZnO nano particles / Aluminium. The substrates were cleaned with Hellmanex III and deionized water in sonication bath for 10 min and the substrates were washed with deionized water two times in sonication bath. Lastly, the substrates were washed with isopropanol in an ultrasonic bath for 10 min. Then the substrates were dried with nitrogen gas flow. The cleaned substrates were then placed into an oxygen plasma device for 15 min. At the same time, PEDOT:PSS was sonicated for 10 min and filtered. The substrates were spin-coated by PEDOT:PSS at 1500 rpm for 1 min and were annealed at 150 °C for 15 min. After that, the substrates were placed

in a glove box and all the next steps were performed under inert conditions. In the glove box, the substrates were annealed for additional 5 min at 150 °C. PVK in chlorobenzene (6 mg/ml) was spin-coated at 3000 rpm for 1 min. After the substrates were annealed at 150 °C for 30 min, QDs in toluene (20 mg/mL) were spin-coated at 1500 rpm for 30 sec. After the substrates were annealed at 60 °C for 15 min, ZnO nanoparticles in ethanol (30 mg/mL) were spin-coated at 2000 rpm for 1 min and the substrates were annealed at 80 °C for 30 min. Then, the substrates were placed in a thermal evaporator with a cathode mask and Al (100 nm) was deposited.

## 3.6 Synthesis of InP Based QDs

### 3.6.1 Synthesis of Green-Emitting InPZnS/Zns QDs

A modified method is used for the synthesis. Some parts of the synthesis method was adapted from the references [10], [59] and [60]. 0.6 mmol of indium (III) acetate ($InAc_3$), 1.8 mmol of myristic acid (MA) and 20 mL of ODE were mixed in a 3-neck flask. The mixture was heated to 100 °C and stirred under vacuum for an hour. After complete dissolution, it was cooled down to room temperature under Ar. Then, 0.2 mmol of zinc stearate (Zn-ste) and 0.025 mmol of 1-dodecanethiol (DDT) were added into flask. Since new materials were loaded to flask, the inert atmosphere of the flask exposed to room air. So the flask was vacuumed and filled with Ar again. Next, the mixture was heated to 220 °C under Ar gas. At that temperature, a solution of 0.08 mmol of $(TMS)_3P$ and 1 mL of ODE, prepared in a glovebox, was swiftly injected into flask. Then the mixture was quickly heated to 285 °C. After 10 min of alloy growth, the flask was cooled down to room temperature. Then, 1 mmol of Zn-ste was added into flask and the mixture was heated to 230 °C under Ar. After 3 h, a solution of 2 mmol of DDT and 1 mL of ODE was added dropwise into flask and maintained for 30 min at 230 °C. For purification, the reaction mixture was centrifuged in order to get rid of the unreacted and agglomerated materials. Then, the QDs were precipitated by adding excess of methanol, acetone and then dispersed in hexane.

### 3.6.2 Synthesis of Red-Emitting InP/Zns QDs

The QDs were synthesized according to literature methods in the references [60], [61]. 0.45 mmol of $InCl_3$, 2.2 mmol of $ZnCl_3$ and 5 mL of oleylamine were mixed in a 3-neck flask. The mixture was heated to 120 °C and stirred under vacuum for an hour. Then, heated to 180 °C under Ar. At that temperature, 0.25 mL of tris(diethylamino)phosphine was swiftly injected into flask. After 20 min, 1 mL of a stock solution of 0.72 g of S dissolved in 10 mL of TOP (2.2 M TOP-S) was slowly added. After 40 min, temperature was raised to 200 °C. After 1 h, a solution of 1 g of Zn-ste dissolved in 4 mL of ODE was added slowly and the mixture was heated to 220 °C. After 30 min, 1 mL of TOP-S stock solution was added slowly and temperature was set to 240 °C. After 30 min, a solution of 0.5 g of Zn-ste dissolved in 2 mL of ODE was added slowly and the mixture was heated to 260 °C. After 30 min, 0.7 mL of TOP-S stock solution was added slowly and the mixture was heated to 280 °C. After 30 min, a solution of 0.5 g of Zn-ste dissolved in 2 mL of ODE was added slowly and set to 300 °C. After 20 min, the reaction was terminated by cooling down. The purification was done using the same method followed during the synthesis of green QDs.

## 3.7 Polymer Film Preparation and Fixing on the QLED

For polymer film, 26% w/v of polystyrene in chloroform solution was prepared. 1 mg of red QDs, 48 mg of green QDs and 0.8 mL of polystyrene-chloroform solution were mixed. The mixture was degassed for a short period of time to get rid of air bubbles and then, drop casted on a clean glass surface. After 24 h, polymer film was peeled off from the glass surface and placed on the PET QLED surface by UV-curable epoxy. For the Förster resonance energy transfer (FRET) control samples, a red polymer film was drop casted by 1 mg of red QDs and 0.8 mL of ps solution, and a green polymer film was drop casted by 48 mg of green QDs and 0.8 mL of polystyrene solution separately.

## 3.8 Characterization and Equipment

The optical characterizations of colloidal quantum dots were carried out by using Agilent-Cary Eclipse Fluorescence Spectrophotometer for photoluminescence measurements, Genesys 10S UV-Vis Spectrophotometer for absorption and Picoquant Fluotime 200 for time resolved photoluminescence measurements. The images of the instruments can be seen in Figure. 3.8.1.

The characterization measurements of the quantum dot light emitting diodes were performed by using an integrated external quantum efficiency measurement system C9920-12 of Hamamatsu. The system employs a Keithley 2400 source meter for the current supply to QLEDs, an integrating sphere for absolute measurement of the emitted light from QLEDs, a photonic multichannel analyser called PMA-12 as a high sensitive photon detector, a halogen lamp for self-absorption correction calculation and a computer with a dedicated software for making all the calculations and instantly display measurement results in the graphics form. The image of the system is given in the Figure. 3.8.2.

The fabrication of the light emitting diodes were performed in a thermal evaporator integrated inert glove box. The pictures of the system are given in the Figure. 3.8.3.

The chemical syntheses of the colloidal nanocrystals are performed with a schlenk line system in a fume hood as given in the Figure. 3.8.4.

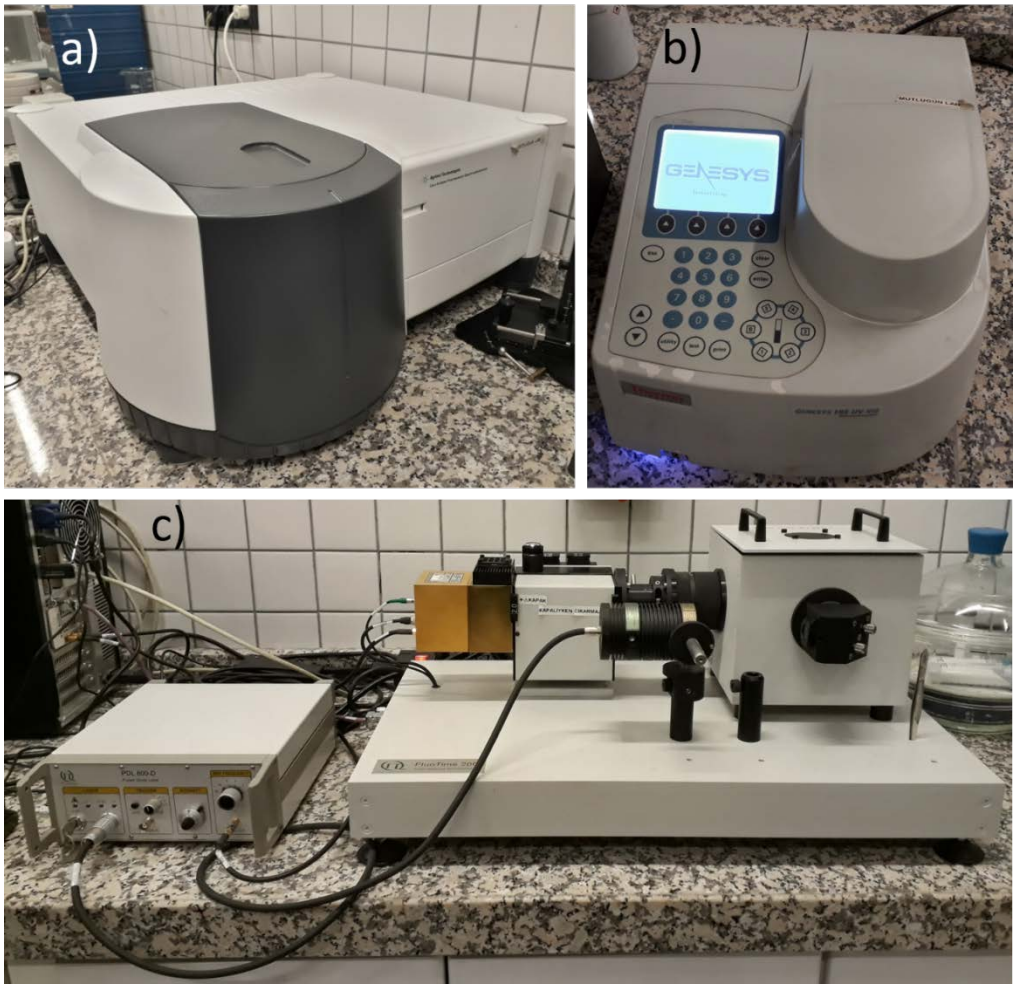


Figure. 3.8.1 Optical characterization instruments for nanocrystals: a) Agilent-Cary Eclipse Fluorescence Spectrophotometer, b) Genesys 10S UV-Vis Spectrophotometer, c) Picoquant Fluotime 200 time resolved spectrometer with PDL 800-D pulsed diode LASER.

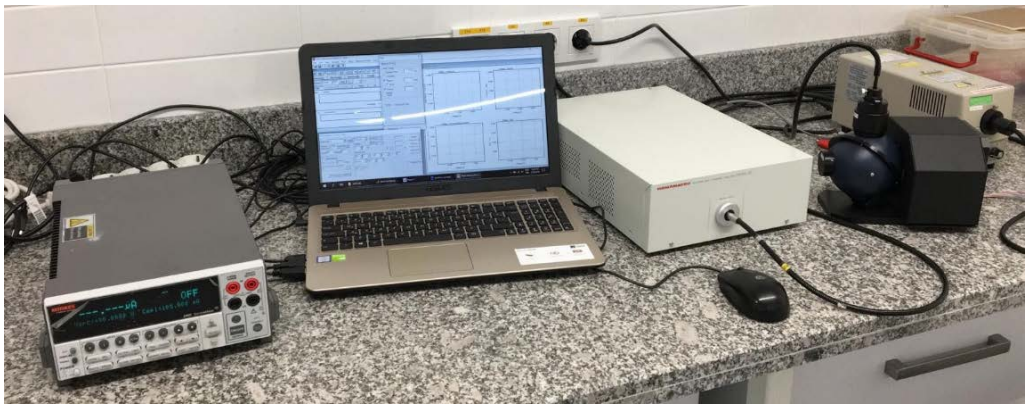

Figure. 3.8.2 The external quantum efficiency measurement system C9920-12 for light emitting diodes. From left to right: Keithley 2400, PC with dedicated software, PMA-12, integrating sphere and halogen light source.


Figure. 3.8.3 The thermal evaporation system integrated to the inert glove box

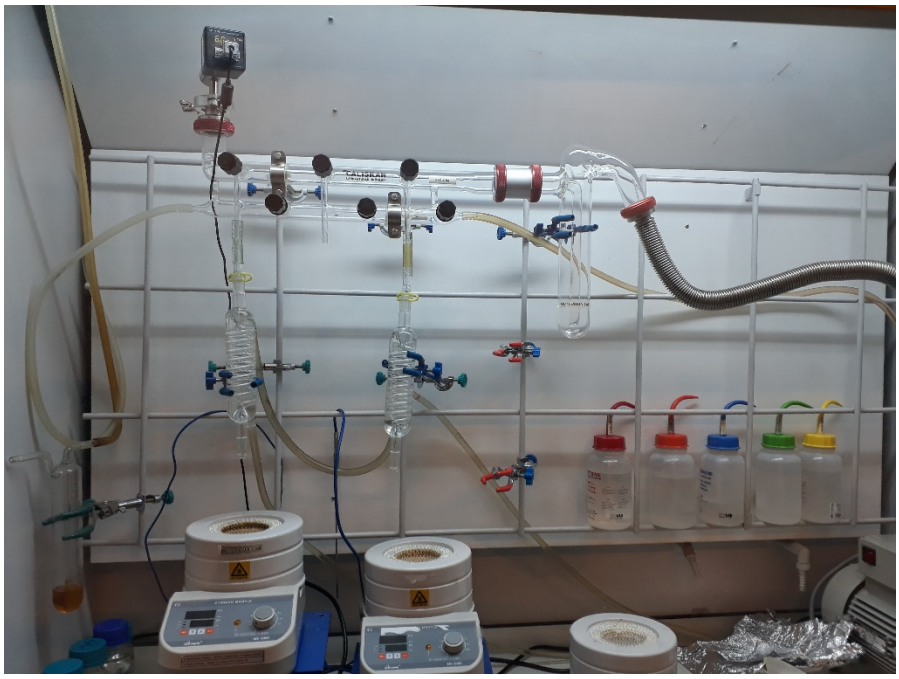

Figure. 3.8.4 The colloidal nanocrystals synthesis system in a fume hood

# Chapter 4

# Results and Discussion

## 4.1 Perovskite Nanocrystals

The syntheses of green $CsPbBr_3$ and red $CsPb(Br_{0.33}/I_{0.67})_3$ nanocrystals were made according to ref. [12] and [54] with slight modifications. First of all, Cs-oleate was prepared. A mixture of $Cs_2CO_3$, octadecene (ODE) and oleic acid (OA) was dried under vacuum for 1 hour at 120 °C. Then the mixture flask was refilled with inert gas argon. Under inert gas, the mixture was heated to 150 °C and kept at that temperature until all $Cs_2CO_3$ reacted with OA. For the perovskite syntheses, a total of 0.187 mmol lead halides mixture or only one type of lead halide, e.g. for green perovskite, only $PbBr_2$; for red perovskite $PbBr_2$ and $PbI_2$ mixture with the ratio of 1:2, and ODE in a flask were dried under vacuum for 1 hour at 120 °C. Then the flask was refilled with argon. At the same temperature, OA and oleylamine (OLA) were injected to flask. The mixture was heated to 160 °C for red perovskite nanocrystals and 180 °C for green perovskite nanocrystals. After the complete solubilisation, Cs-oleate was swiftly injected to flask and 5 seconds later, the mixture was cooled by an ethanol bath. The schematic descriptions of the syntheses of red and green perovskite nanocrystals can be seen in the Figure. 4.1.1.

The purification of perovskite nanocrystals was done according to a hybrid method. The purification method in the reference [12] is based on only centrifugation. However, only centrifugation is not generally sufficient to separate nano-sized particles from a solvent such as ODE. Therefore, during the purification of the semiconductor nanocrystals (e.g. cadmium based quantum dots), precipitants such as acetone, ethanol, and methanol are used extensively, together with the centrifugation. Unfortunately, these classical precipitants are too destructive for the delicate nature of the perovskite nanocrystals. In the purification method of the reference [54], acetone was, indeed, used as the precipitant but, with a heavy precaution of the addition of the excess amount of OA and OLA ligands, just before the introduction of the acetone. Although the resultant perovskite nanocrystals are of high photoluminescence quantum yield (PLQY), their application in a light emitting device is not that much promising. Because the charge injection is very limited over the excess dielectric ligands into the perovskite nanocrystal core. Moreover, the effectiveness of this method of addition of the excess ligands, before the addition of the acetone as the precipitant is very limited with the use of only the green $CsPbBr_3$ perovskite nanocrystals. The application of this purification method to an iodine (I) containing perovskite nanocrystal results with the loss of the I elements, so the color, and even the structural integrity of the nanocrystal. In addition to all of these, the reference in question offers a remarkable purification route consists of three stage centrifugation. At the first step, the reaction solution was centrifuged to discard most of the ODE and unreacted residuals. The precipitate was dispersed in hexane. At the second step, the suspension was centrifuged to discard larger nanocrystals and agglomerates. This time, the supernatant was taken. The excess ligands of OA and OLA was added to supernatant. At the last step, the suspension was centrifuged as soon as the acetone was added. On the other hand, as a suitable precipitant, the ethyl acetate was proposed in the reference [29]. Compared to classical quantum dots, perovskite nanocrystals are more ionic in nature. Thus, they are sensitive to many polar solvents. The main reason of the sensitivity of the perovskite nanocrystals to the classical precipitants, mentioned above, is the polarity of the precipitants. So the non-polar ethyl acetate is one of the ideal solvents for precipitating the perovskite nanocrystals.

It has always been a problem to purify perovskite nanocrystals. Especially it is harder, if the perovskite nanocrystals are synthesized to be used in a light emitting diode. In order to overcome the problems and benefit from the literature as much as

possible, a hybrid method was used. As in the ref. [53], a three stage of centrifugation method was applied to achieve a better size selective precipitation. However at the last stage, as in the ref. [28], the ethyl acetate was used instead of acetone without the addition of excess ligands. The photoluminescence emission spectra and the absorbance spectra of the purified red and green perovskite nanocrystals can be seen in the Figure. 4.1.2.

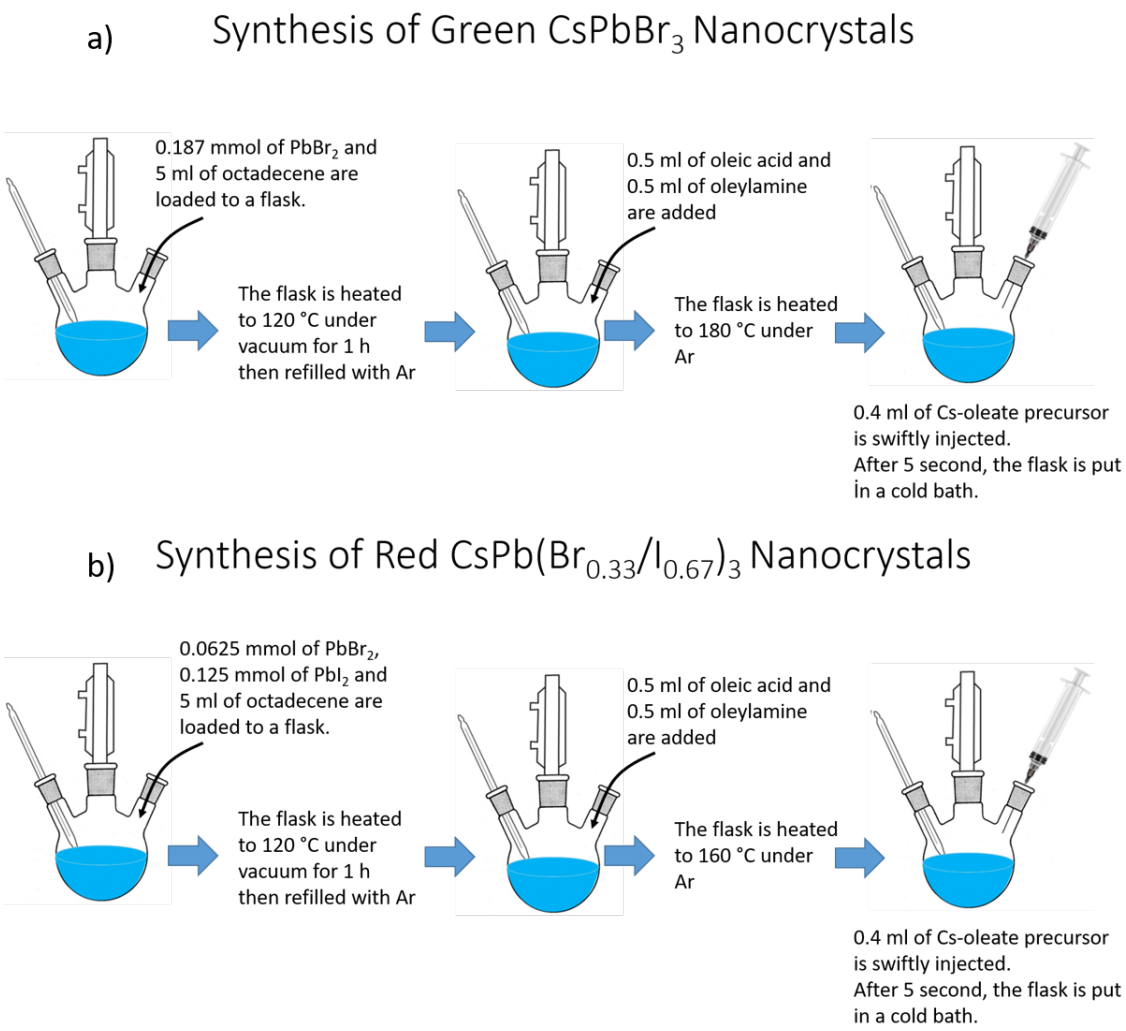


Figure. 4.1.1 The schematic description of a) green perovskite nanocrystals synthesis and b) red perovskite nanocrystal synthesis

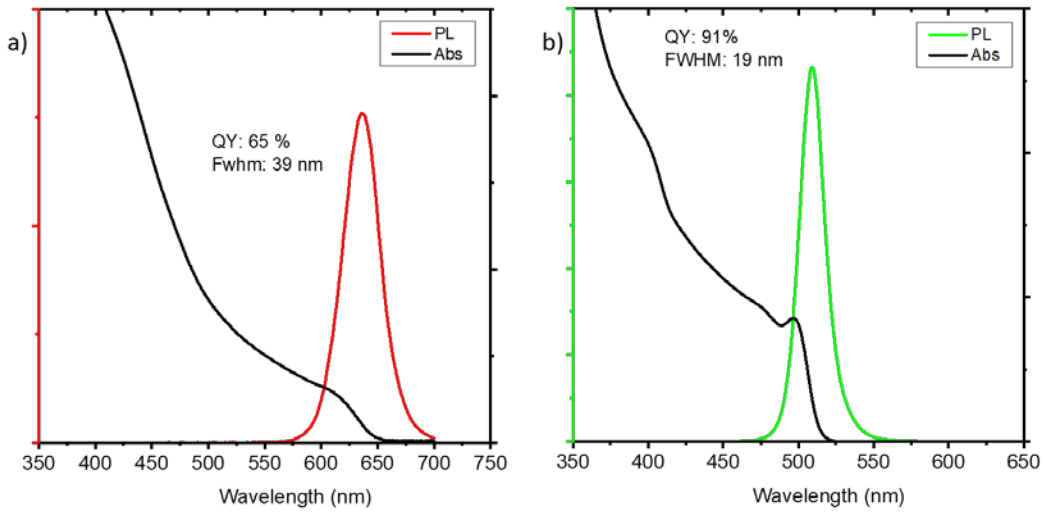


Figure. 4.1.2 The photoluminescence emission spectra and the absorbance spectra of the purified a) red and b) green perovskite nanocrystals

## 4.2 Perovskite Light Emitting Diodes

The colloidal perovskite nanocrystals-based light emitting diode devices were fabricated on ITO coated and patterned glass substrates. On top of the ITO layer poly(ethylenedioxythiophene):polystyrene sulfonate (PEDOT:PSS), Poly(N,N'-bis-4-butylphenyl-N,N'-bisphenyl)benzidine (Poly-TPD) in chlorobenzene and colloidal perovskite nanocrystals in octane layers were spin coated. After the perovskite nanocrystals layer, in order to avoid from damaging the layer, a physical vapour deposition method was used instead of spin coating. The 2,2',2''-(1,3,5-Benzinetriyl)-tris(1-phenyl-1-H-benzimidazole) (TPBi), lithium fluoride (LiF) and aluminium (Al) layers were thermally evaporated in a high vacuum chamber integrated into an inert glove box. (Figure. 3.8.3 for the thermal evaporation system and the glove box; Figure. 4.2.1 for the fabrication schematics of a perovskite light emitting diode.) Then the device was encapsulated with epoxy resin and a piece of glass before characterization.

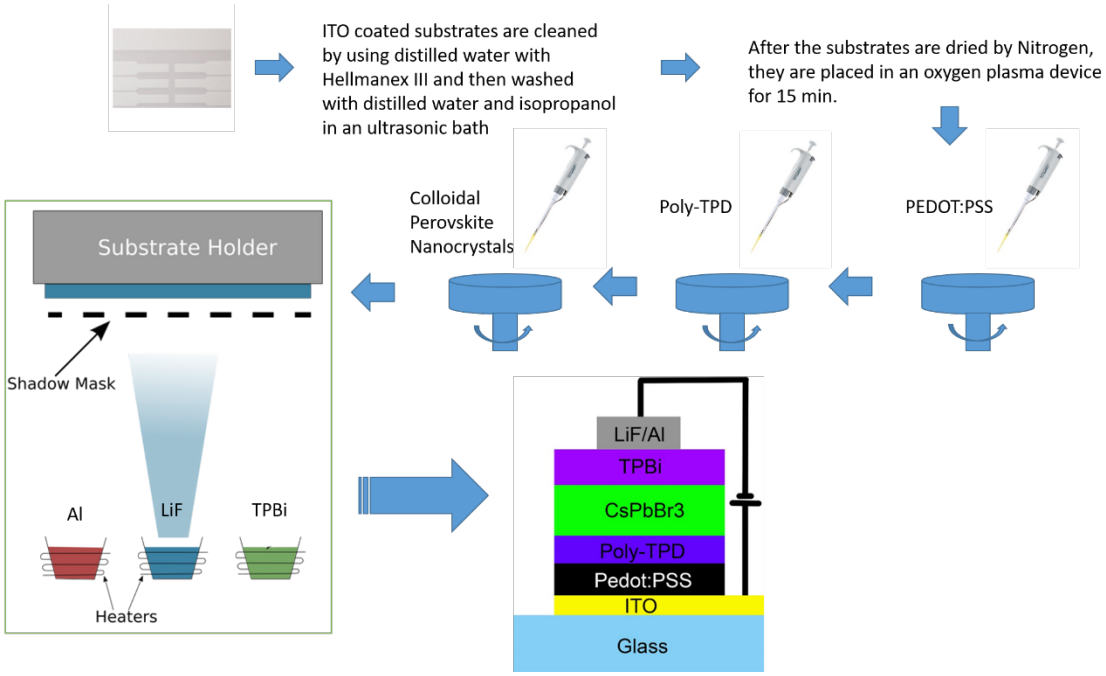


Figure. 4.2.1 The schematic description of fabrication of a perovskite light emitting diode, starting from the top left substrate cleaning, spin coating and thermal evaporation to final device at the bottom middle with the guidance of the arrows

| Layer | Solvent | Density (mg/ml) | Spin-c. RPM | Spin-c. Dur. | Baking Temp. | Baking Dur. |
|---|---|---|---|---|---|---|
| PEDOT:PSS | | | 2000 | 1 min | 150 °C | 20 min |
| Poly-TPD | Chlorobenzene | 5 | 4000 | 1 min | 120 °C | 15 min |
| Poly-TPD | Chlorobenzene | 7.5 | 4000 | 1 min | 120 °C | 15 min |
| Poly-TPD | Chlorobenzene | 10 | 4000 | 1 min | 120 °C | 15 min |
| Poly-TPD | Chlorobenzene | 15 | 4000 | 1 min | 120 °C | 15 min |
| $CsPb(Br/I)_3$ (Red) | Hexane | 10 | 4000 | 1 min | 60 °C | 15 min |
| $CsPb(Br/I)_3$ (Red) | Hexane | 15 | 4000 | 1 min | 60 °C | 15 min |
| $CsPb(Br/I)_3$ (Red) | Octane | 10 | 4000 | 1 min | 60 °C | 15 min |
| $CsPb(Br/I)_3$ (Red) | Octane | 15 | 4000 | 1 min | 60 °C | 15 min |
| $CsPb(Br)_3$ (Green) | Hexane | 10 | 4000 | 1 min | 60 °C | 15 min |

Table 4.2.1 The table of the coating parameters of the spin coated layers. The combinations of the different parameters of Poly-TPD and perovskite layers were studied. Green rows happened to be the most optimized parameters according to characterizations.

The fabrication of a light emitting diode device has been performed for the first time in the Abdullah Gül University within the scope of this thesis. Therefore, the whole thesis should be considered as an optimization study for the inception of the fabrication and the characterization of the nanocrystals based light emitting diodes. As mentioned in the Chapter 2, the initial optimization studies of the light emitting diodes were based on the relatively stable, classical semiconductor based nanocrystals such as CdSe/ZnS quantum dots. Those studies have shown that the parameters of the emissive layer has the biggest effect on the LED device, as the name implies. Thus, the optimizations of the perovskite nanocrystals based light emitting diodes also focused on the emissive layer, at first. The most suitable solvent and the density of the colloidal perovskite nanocrystals were determined by experiments. After the optimization of the emissive layer, based on the characterization results, the hole transport layer of Poly-TPD was optimized. While these two spin coated layers were being studied, the parameters of the thermally evaporated layers were kept constant at 0.193 kÅ for TPBi, 0.001 kÅ for LiF and 1 kÅ for Al. The parameters studied for the spin coated layers are presented in the Table 4.2.1. In the table, the green rows represent the most optimized parameters. The best results were achieved with the spin coating of 10 mg/ml Poly-TPD dissolved in chlorobenzene at 4000 rpm, 10 mg/ml $CsPb(Br/I)_3$ dispersed in octane at 4000 rpm. The best device emitting at 649.9 nm has an external quantum efficiency (EQE) of 1.572 %, a luminance of 601 $cd/m^2$, and a $V_{turn\text{-}on}$ of 6.2 V (Figure. 4.2.2).

As the solvent for the colloidal perovskite nanocrystals, two different solvents were experimentally studied. The first one is the hexane which is a favourite solvent used in syntheses for the colloidal stability. The second one is the octane which was offered in the literature articles frequently for the solution processing of the colloidal perovskite nanocrystals. The other options such as toluene, chloroform, chlorobenzene etc. were eliminated, because of the stability problems known from the early synthesis and film studies.

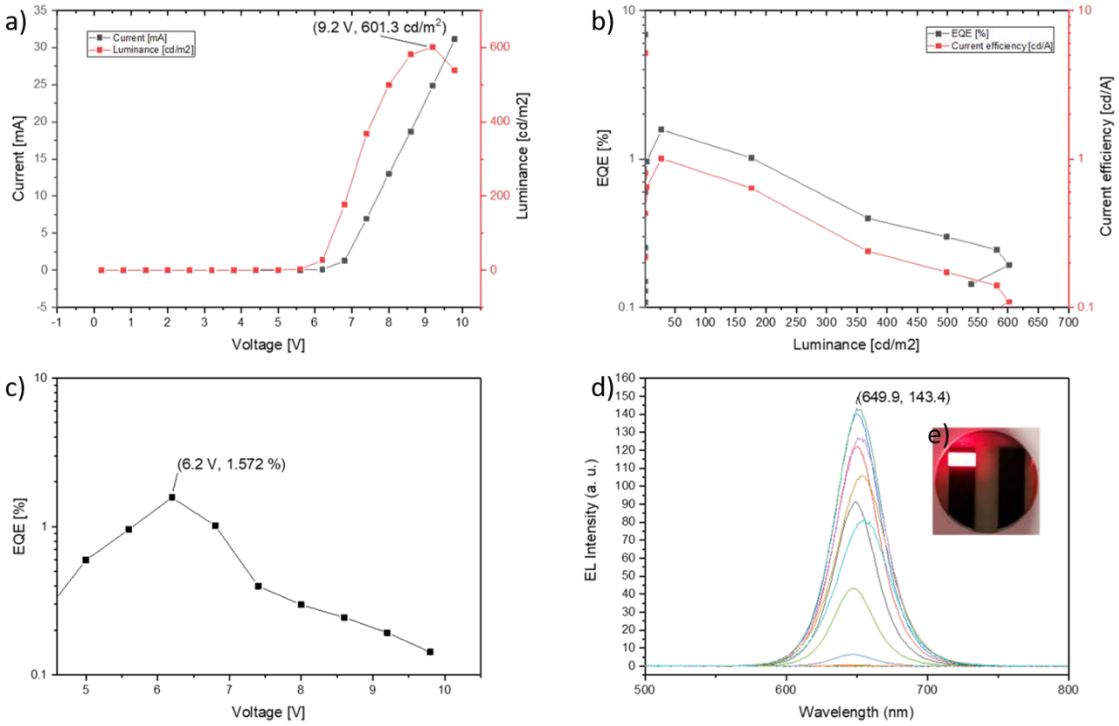


Figure. 4.2.2 The measurement results of the best performing light emitting diode based on $CsPB(Br/I)_3$ red perovskite nanocrystals. a) voltage vs. current and voltage vs. luminance, b) luminance vs. external quantum efficiency (EQE) and luminance vs. current efficiency, c) voltage vs. EQE, d) emission spectra of the LED at different voltages, e) the photograph of the LED

Even during the experiments, it could be expected that the octane would perform better because the spin coated films of perovskite nanocrystals from hexane were so rough that the roughness could even be seen with eyes. On the other hand the films spin coated from octane solution had a smoother surface. The characterization results were consistent with the observations. According to the results, the hexane based LEDs had an average external quantum efficiency (EQE) of 0.55 %, but the octane based LEDs had an average EQE of 1.235 %.

After determining the solvent type as the octane, the density of the colloidal perovskite nanocrystal solution was studied. The density of the solution which is going to be spin-coated affects directly the thickness of the layer, together with the spin speed. The two different density values of 10 and 15 mg/ml were compared according to characterization results of the LED devices. The results of the fabricated LEDs showed that, the two of them had a similar average EQE and a maximum EQE value but, 10 mg/ml based LEDs had an average luminance value of 460 $cd/m^2$, while 15 mg/ml based LEDs had an average luminance value of 383 $cd/m^2$ (Table 4.2.2). However all of

the QLEDs, until this stage, had a very high turn on voltage of typically 8.5 V. In addition to that, the emission spectra of the QLEDs, generally, had a tail at the left hand side of the graph, attributed to Poly-TPD emission. It was an undesired emission and pointed out an unbalanced charge injection which means that the holes were slower when compared to the electrons. In order to lower the turn on voltage and increase the charge balance, the experiments aimed to optimise the hole transport layer of Poly-TPD. In order to inject holes faster, the Poly-TPD layer thickness was decreased by diluting the Poly-TPD solution in chlorobenzene from 15 mg/ml to 10, 7.5 and 5 mg/ml. The results show that diluting the Poly-TPD solution decreased the turn-on voltage from very high, unpractical value of 8.5 V to practical levels of 3.8 to 4.8 V, along with the purer emission spectra and, the 10 mg/ml based LED devices had the highest average EQE value of 1.508 % (Table 4.2.3). This device also corresponds to the green rows in the Table 4.2.1 and the LED whose results are presented in the Figure. 4.2.2.

The measurement graphics of the characterizations of the other devices during the optimization experiments can be seen in the Figures from 4.2.3 to 4.2.8. In addition to these red perovskite light emitting diodes, the measurement results of a green emitting perovskite LED which was fabricated by using hexane can be seen in the Figure. 4.2.9. The poor results of the green perovskite LED are consistent with the other red perovskite LEDs which were fabricated by using hexane.

| density / solvent | 10 mg/ml | 15 mg/ml |
|---|---|---|
| Octane (dried) | $EQE_{max}$: 1.316 %<br>$EQE_{avg}$: 1.235 %<br>$L_{max}$: 487 cd/m$^2$<br>$L_{avg}$: 460 cd/m$^2$ | $EQE_{max}$: 1.283 %<br>$EQE_{avg}$: 1.241 %<br>$L_{max}$: 420 cd/m$^2$<br>$L_{avg}$: 383 cd/m$^2$ |
| Hexane (dried) | $EQE_{max}$: 1.164 %<br>$EQE_{avg}$: 0.55 %<br>$L_{max}$: 282 cd/m$^2$<br>$L_{avg}$: 211 cd/m$^2$ | $EQE_{max}$: 0.934 %<br>$EQE_{avg}$: 0.609 %<br>$L_{max}$: 265 cd/m$^2$<br>$L_{avg}$: 224 cd/m$^2$ |

Table 4.2.2 The table shows the numeric results of the characterizations of the perovskite nanocrystal based light emitting diode devices fabricated for the experimental optimizations of the emissive layer (perovskite nanocrystals)

| P-TPD density / solvent | 5 mg/ml | 7.5 mg/ml | 10 mg/ml |
|---|---|---|---|
| Chlorobenzene | $EQE_{max}$: 1.339 %<br>$EQE_{ort}$: 1.199 %<br>$L_{max}$: 373 cd/m$^2$<br>$L_{ort}$: 343 cd/m$^2$<br>$V_{turn-on}$: 3.8 V | $EQE_{max}$: 1.591 %<br>$EQE_{ort}$: 1.316 %<br>$L_{max}$: 492 cd/m$^2$<br>$L_{ort}$: 457 cd/m$^2$<br>$V_{turn-on}$: 4.4 V | $EQE_{max}$: 1.572 %<br>$EQE_{ort}$: 1.508 %<br>$L_{max}$: 601 cd/m$^2$<br>$L_{ort}$: 585 cd/m$^2$<br>$V_{turn-on}$: 4,8 V |

Table 4.2.3 The table shows the numeric results of the characterizations of the perovskite nanocrystal based light emitting diode devices fabricated for the experimental optimizations of hole transport layer (Poly-TPD)

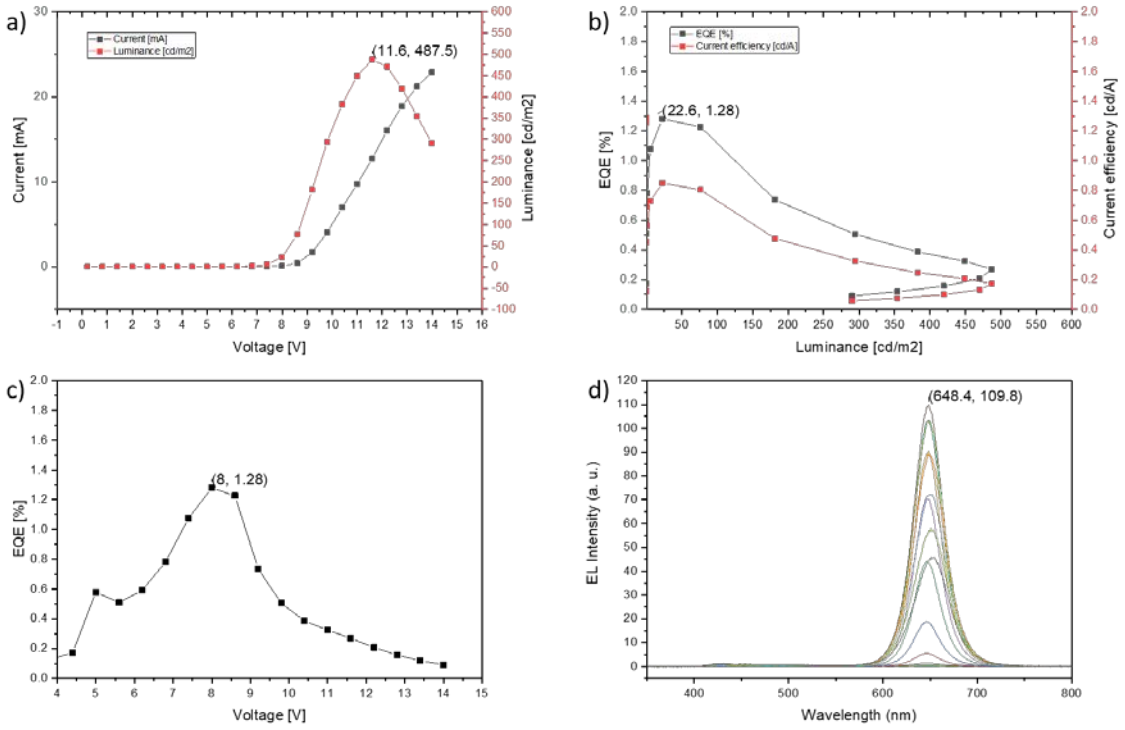


Figure. 4.2.3 The measurement results of the red perovskite LED: Perovskite in octane 10 mg/ml, Poly-TPD 15 mg/ml. a) voltage vs. current and voltage vs. luminance, b) luminance vs. external quantum efficiency (EQE) and luminance vs. current efficiency, c) voltage vs. EQE, d) emission spectra of the LED at different voltages

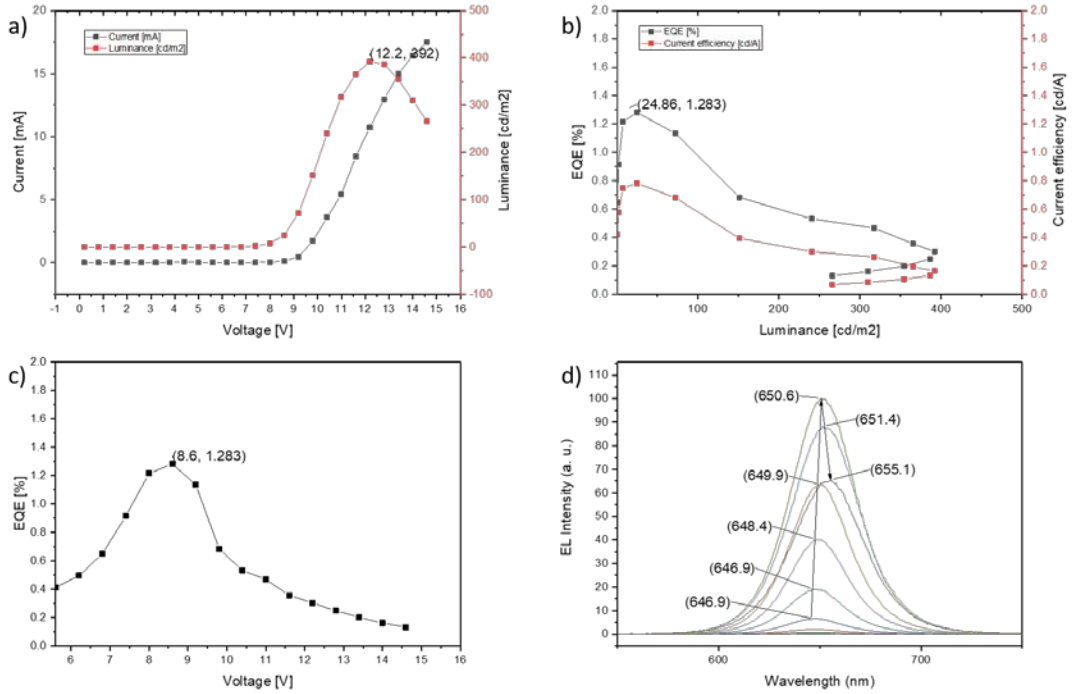


Figure. 4.2.4 The measurement results of the red perovskite LED: Perovskite in octane 15 mg/ml, Poly-TPD 15 mg/ml. a) voltage vs. current and voltage vs. luminance, b) luminance vs. external quantum efficiency (EQE) and luminance vs. current efficiency, c) voltage vs. EQE, d) emission spectra of the LED at different voltages

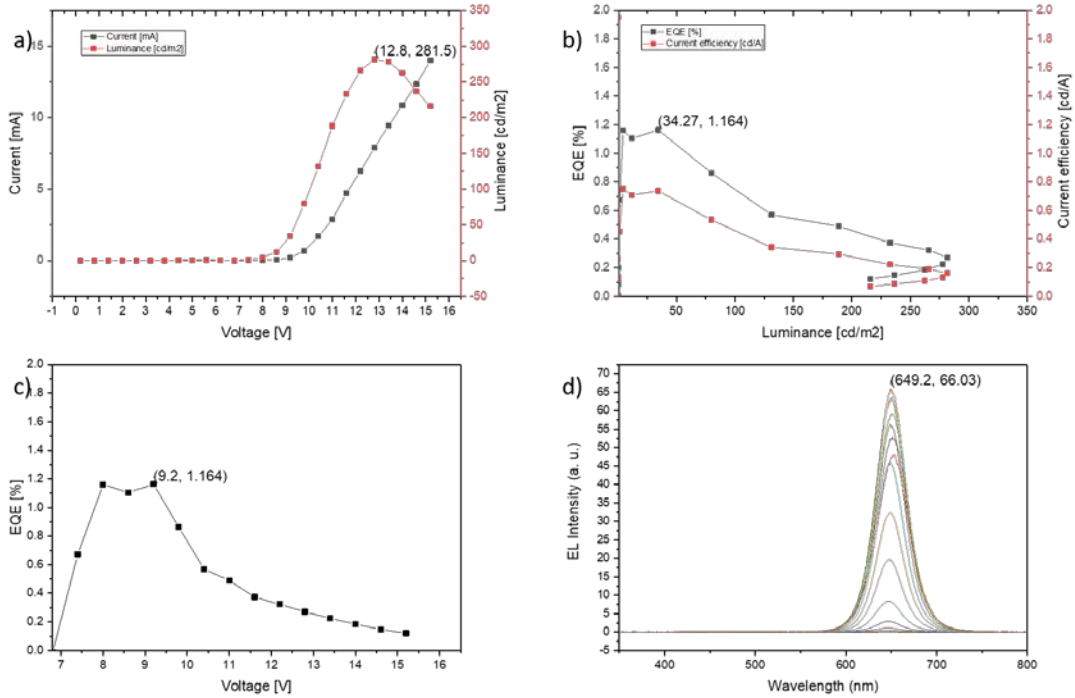


Figure. 4.2.5 The measurement results of the red perovskite LED: Perovskite in hexane 10 mg/ml, Poly-TPD 15 mg/ml. a) voltage vs. current and voltage vs. luminance, b) luminance vs. external quantum efficiency (EQE) and luminance vs. current efficiency, c) voltage vs. EQE, d) emission spectra of the LED at different voltages

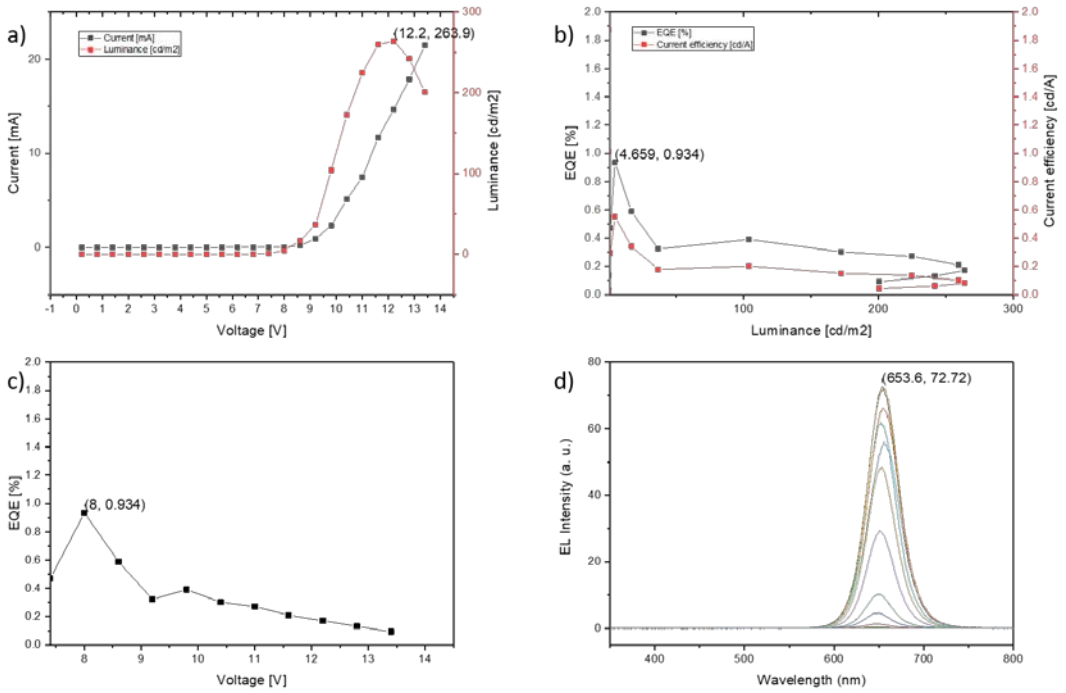


Figure. 4.2.6 The measurement results of the red perovskite LED: Perovskite in hexane 15 mg/ml, Poly-TPD 15 mg/ml. a) voltage vs. current and voltage vs. luminance, b) luminance vs. external quantum efficiency (EQE) and luminance vs. current efficiency, c) voltage vs. EQE, d) emission spectra of the LED at different voltages

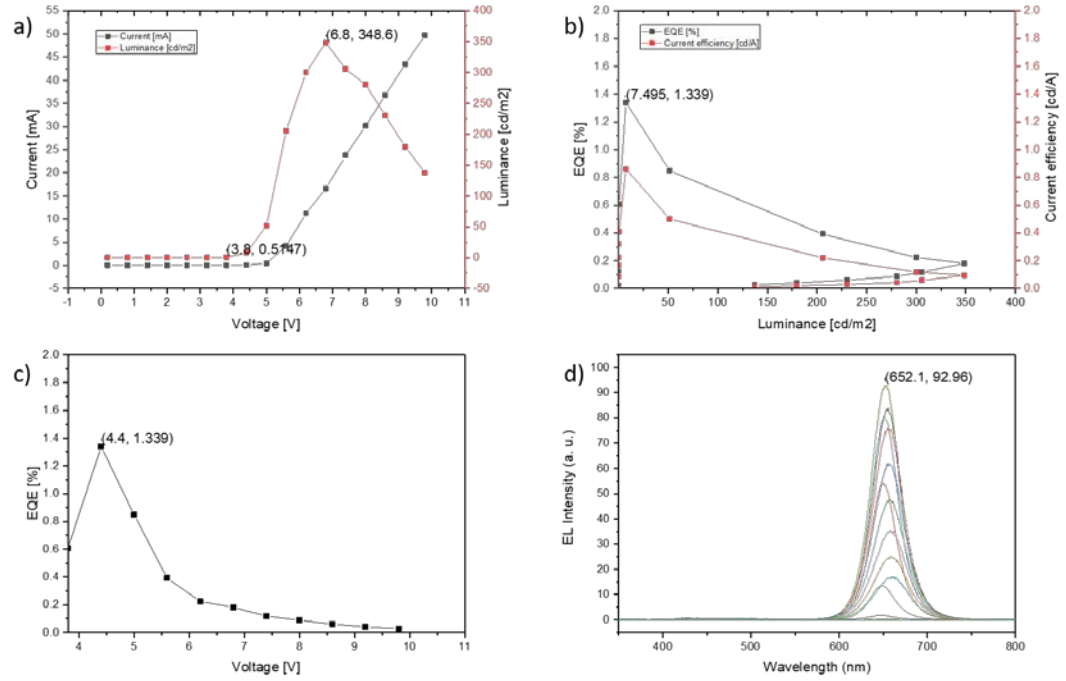


Figure. 4.2.7 The measurement results of the red perovskite LED: Perovskite in octane 10 mg/ml, Poly-TPD 5 mg/ml. a) voltage vs. current and voltage vs. luminance, b) luminance vs. external quantum efficiency (EQE) and luminance vs. current efficiency, c) voltage vs. EQE, d) emission spectra of the LED at different voltages

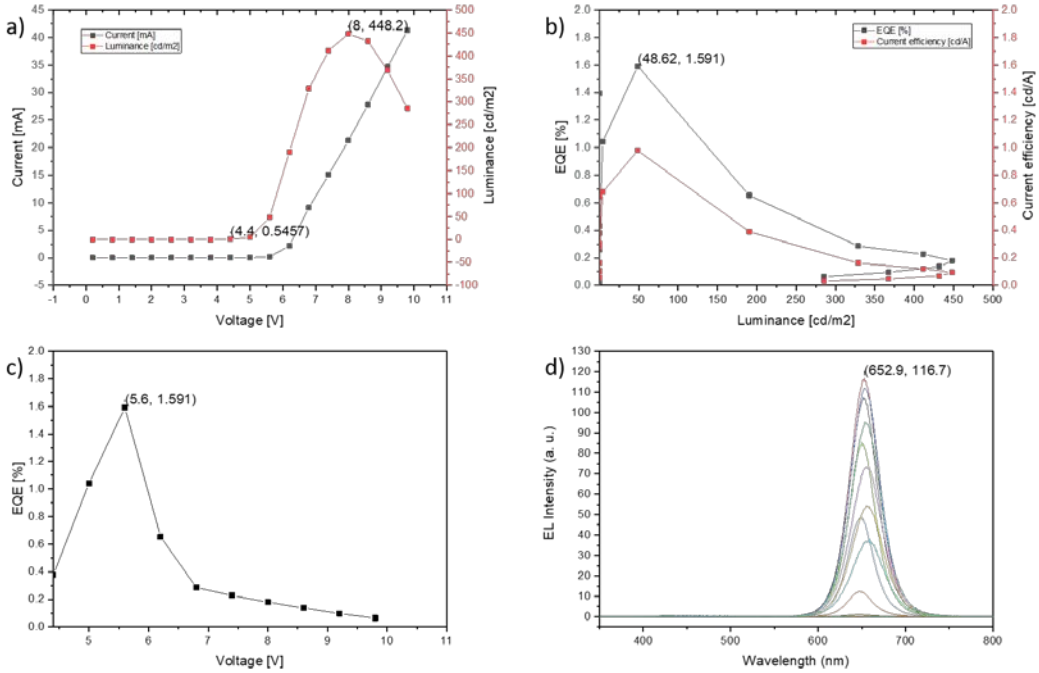


Figure. 4.2.8 The measurement results of the red perovskite LED: Perovskite in octane 10 mg/ml, Poly-TPD 7.5 mg/ml. a) voltage vs. current and voltage vs. luminance, b) luminance vs. external quantum efficiency (EQE) and luminance vs. current efficiency, c) voltage vs. EQE, d) emission spectra of the LED at different voltages

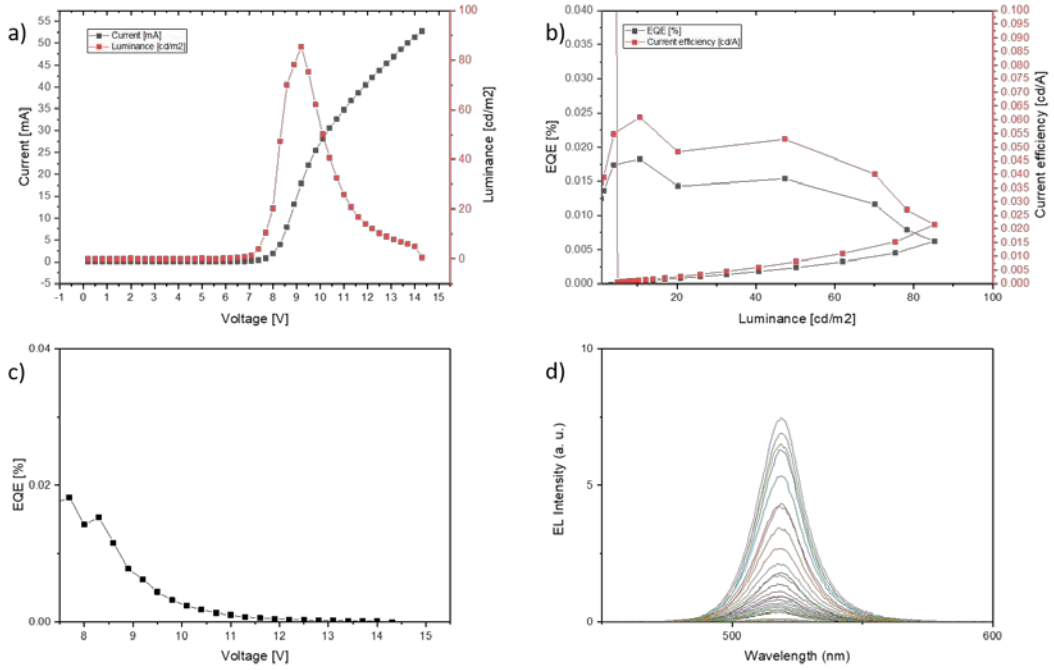


Figure. 4.2.9 The measurement results of the green perovskite LED: Perovskite in hexane 10 mg/ml, Poly-TPD 15 mg/ml. a) voltage vs. current and voltage vs. luminance, b) luminance vs. external quantum efficiency (EQE) and luminance vs. current efficiency, c) voltage vs. EQE, d) emission spectra of the LED at different voltages

These results show that there is a need for more research on the perovskite nanocrystal based light emitting diodes. The efficiencies are quite poor when compared to Cd based QLEDs. One of the main reason of this is the instability of perovskite nanocrystals. The instability makes it almost impossible to spin coat on top of the perovskite layer. For this reason, the new generation inorganic electron transport layer materials such as ZnO nanoparticles are nearly impossible to use in the perovskite nanocrystal light emitting diodes. However, it is known that the inorganic electron transport layers are the one of the biggest factor of recently increasing performances of Cd based light emitting diodes. Because their band levels and gaps are optimum in most cases and even it is possible to tune them by doping. Additionally, inorganic materials are more resistive to oxygen and moisture caused degradations. Moreover, they are not just stable but also they increase the stability of the quantum dot layer underneath them by covering and saving them from unpleasing factors of atmosphere.

# Chapter 5

# Conclusions and Future Perspective

The colloidal perovskite nanocrystals have unique optoelectronic features such as near-unity efficiency, narrow emission linewidth, solution processability and compatibility with flexible electronics. Recently, with these features, they collected interests of research efforts. The ability of tuning the emission wavelength by adjusting the composition ratio of halides is a fantastic property. However there are still big issues about this feature because, it is too easy to exchange anions unwillingly. For example, a mixed halide perovskite can change its color in time or with the amount of applied voltage. That makes mixed halide perovskite nanocrystals based light emitting diodes unstable in terms of emission color. Moreover, the halides can be lost quickly. If this happens the perovskite nanocrystals become dead. Due to this problem, it is so hard to spin coat a layer onto perovskite quantum dot layer. Almost all orthogonal solvents for perovskite quantum dots etch halides and kill them. This problem mandates to use organic electron transport layers instead of inorganic ones which limits the performance of perovskite nanocrystals-based LEDs the most. Another problem for the perovskite nanocrystals is the excess ligands. The ligands are the only agents which protect the perovskites. The ligands prevents them to be aggregated or lost the halides when the perovskites nanocrystals in the form of a thin film. However, the ligands are highly

resistive organic molecules which makes it hard to inject charge carriers into the perovskite nanocrystals. If an effective encapsulation or a kind of shell chemistry is developed for the perovskite nanocrystals in the future, most of these problems will be solved. The other issue to be resolved is the toxic effects of the lead. It may exceed the limits in most applications. However this problem can, hopefully, be overcome by studying the crystal chemistry of the perovskite in the search for a suitable element to replace the lead.

Still, the perovskite nanocrystals promise a bright future in terms of new generation displays and light emitting diodes. I hope that my little contribution to the topic will have a positive effect on the future researches.

# BIBLIOGRAPHY


[1] A. Ekimov, A. Onushchenko, “Quantum size effect in three-dimensional microscopic semiconductor crystals,” Soviet Journal of Experimental and Theoretical Physics Letters, 34, 345 (1981).

[2] A. Henglein, “Photo-Degradation and Fluorescence of Colloidal-Cadmium Sulfide in Aqueous Solution,” Berichte der Bunsengesellschaft für physikalische Chemie, 86, 301 (1982).

[3] L. E. Brus, “Electron–electron and electron-hole interactions in small semiconductor crystallites: The size dependence of the lowest excited electronic state,” The Journal of Chemical Physics, 80, 4403 (1984).

[4] M. A. Hines, P. Guyot-Sionnest, “Synthesis and Characterization of Strongly Luminescing ZnS-Capped CdSe Nanocrystals,” The Journal of Physical Chemistry, 100, 468 (1996).

[5] O. Chen, J. Zhao, V. P. Chauhan, J. Cui, C. Wong, D. K. Harris, H. Wei, H.-S. Han, D. Fukumura, R. K. Jain, M. G. Bawendi, “Compact high-quality CdSe–CdS core–shell nanocrystals with narrow emission linewidths and suppressed blinking,” Nature Materials, 12, 445 (2013).

[6] H. Qin, Y. Niu, R. Meng, X. Lin, R. Lai, W. Fang, X. Peng, “Single-Dot Spectroscopy of Zinc-Blende CdSe/CdS Core/Shell Nanocrystals: Nonblinking and Correlation with Ensemble Measurements,” Journal of the American Chemical Society, 136, 179 (2014).

[7] J. M. Pietryga, Y.-S. Park, J. Lim, A. F. Fidler, W. K. Bae, S. Brovelli, V. I. Klimov, “Spectroscopic and Device Aspects of Nanocrystal Quantum Dots,” Chemical Reviews, 116, 10513 (2016).

[8] A. P. Alivisatos, “Perspectives on the physical chemistry of semiconductor nanocrystals,” Journal of Physical Chemistry, 100, 13226 (1996).

[9] S. Xu, J. Ziegler, T. Nann, “Rapid synthesis of highly luminescent InP and

InP/ZnS nanocrystals," Journal of Materials Chemistry, 18, 2653 (2008).

[10] Y. Altıntas, M. Y. Talpur, E. Mutlugun, "The effect of ligand chain length on the optical properties of alloyed core-shell InPZnS/ZnS quantum dots," Journal of Alloys and Compounds, 711, 335 (2017).

[11] L. C. Schmidt, A. Pertegás, S. González-Carrero, O. Malinkiewicz, S. Agouram, G. Mínguez Espallargas, H. J. Bolink, R. E. Galian, J. Pérez-Prieto, "Nontemplate Synthesis of CH 3 NH 3 PbBr 3 Perovskite Nanoparticles," Journal of the American Chemical Society, 136, 850 (2014).

[12] L. Protesescu, S. Yakunin, M. I. Bodnarchuk, F. Krieg, R. Caputo, C. H. Hendon, R. X. Yang, A. Walsh, M. V. Kovalenko, "Nanocrystals of Cesium Lead Halide Perovskites (CsPbX 3 , X = Cl, Br, and I): Novel Optoelectronic Materials Showing Bright Emission with Wide Color Gamut," Nano Letters, 15, 3692 (2015).

[13] F. Zhang, H. Zhong, C. Chen, X. Wu, X. Hu, H. Huang, J. Han, B. Zou, Y. Dong, "Brightly Luminescent and Color-Tunable Colloidal CH 3 NH 3 PbX 3 (X = Br, I, Cl) Quantum Dots: Potential Alternatives for Display Technology," ACS Nano, 9, 4533 (2015).

[14] L. Protesescu, S. Yakunin, S. Kumar, J. Bär, F. Bertolotti, N. Masciocchi, A. Guagliardi, M. Grotevent, I. Shorubalko, M. I. Bodnarchuk, C.-J. Shih, M. V. Kovalenko, "Dismantling the 'Red Wall' of Colloidal Perovskites: Highly Luminescent Formamidinium and Formamidinium–Cesium Lead Iodide Nanocrystals," ACS Nano, 11, 3119 (2017).

[15] D. Parobek, B. J. Roman, Y. Dong, H. Jin, E. Lee, M. Sheldon, D. H. Son, "Exciton-to-Dopant Energy Transfer in Mn-Doped Cesium Lead Halide Perovskite Nanocrystals," Nano Letters, 16, 7376 (2016).

[16] A. Wang, X. Yan, M. Zhang, S. Sun, M. Yang, W. Shen, X. Pan, P. Wang, Z. Deng, "Controlled Synthesis of Lead-Free and Stable Perovskite Derivative Cs 2 SnI 6 Nanocrystals via a Facile Hot-Injection Process," Chemistry of Materials, 28, 8132 (2016).

[17] R. Roccanova, A. Yangui, H. Nhalil, H. Shi, M.-H. Du, B. Saparov, "Near-Unity Photoluminescence Quantum Yield in Blue-Emitting Cs 3 Cu 2 Br 5– x I x ($0 \leq x \leq 5$)," ACS Applied Electronic Materials, 1, 269 (2019).

[18] G. Nedelcu, L. Protesescu, S. Yakunin, M. I. Bodnarchuk, M. J. Grotevent, M. V. Kovalenko, "Fast Anion-Exchange in Highly Luminescent Nanocrystals of

Cesium Lead Halide Perovskites (CsPbX 3 , X = Cl, Br, I)," Nano Letters, 15, 5635 (2015).

[19] Y. Altintas, I. Torun, A. F. Yazici, E. Beskazak, T. Erdem, M. Serdar Onses, E. Mutlugun, "Multiplexed patterning of cesium lead halide perovskite nanocrystals by additive jet printing for efficient white light generation," Chemical Engineering Journal, 380, 122493 (2020).

[20] E. Jang, S. Jun, H. Jang, J. Lim, B. Kim, Y. Kim, "White-Light-Emitting Diodes with Quantum Dot Color Converters for Display Backlights," Advanced Materials, 22, 3076 (2010).

[21] J. S. Steckel, J. Ho, C. Hamilton, J. Xi, C. Breen, W. Liu, P. Allen, S. Coe-Sullivan, "Quantum dots: The ultimate down-conversion material for LCD displays," Journal of the Society for Information Display, 23, 294 (2015).

[22] Y. Altintas, S. Genc, M. Y. Talpur, E. Mutlugun, "CdSe/ZnS quantum dot films for high performance flexible lighting and display applications," Nanotechnology, 27, 295604 (2016).

[23] Y.-H. Ko, M. Jalalah, S.-J. Lee, J.-G. Park, "Super Ultra-High Resolution Liquid-Crystal-Display Using Perovskite Quantum-Dot Functional Color-Filters," Scientific Reports, 8, 12881 (2018).

[24] V. L. Colvin, M. C. Schlamp, A. P. Alivisatos, "Light-emitting diodes made from cadmium selenide nanocrystals and a semiconducting polymer," Nature, 370, 354 (1994).

[25] O. Wang, L. Wang, Z. Li, Q. Xu, Q. Lin, H. Wang, Z. Du, H. Shen, L. S. Li, "High-efficiency, deep blue ZnCdS/Cd x Zn 1−x S/ZnS quantum-dot-light-emitting devices with an EQE exceeding 18%," Nanoscale, 10, 5650 (2018).

[26] X. Dai, Z. Zhang, Y. Jin, Y. Niu, H. Cao, X. Liang, L. Chen, J. Wang, X. Peng, "Solution-processed, high-performance light-emitting diodes based on quantum dots," Nature, 515, 96 (2014).

[27] H. Zhang, X. Sun, S. Chen, "Over 100 cd A −1 Efficient Quantum Dot Light-Emitting Diodes with Inverted Tandem Structure," Advanced Functional Materials, 27, 1700610 (2017).

[28] J. Song, J. Li, X. Li, L. Xu, Y. Dong, H. Zeng, "Quantum Dot Light-Emitting Diodes Based on Inorganic Perovskite Cesium Lead Halides (CsPbX 3 )," Advanced Materials, 27, 7162 (2015).

[29] J. Li, L. Xu, T. Wang, J. Song, J. Chen, J. Xue, Y. Dong, B. Cai, Q. Shan, B.

Han, H. Zeng, “50-Fold EQE Improvement up to 6.27% of Solution-Processed All-Inorganic Perovskite CsPbBr 3 QLEDs via Surface Ligand Density Control,” Advanced Materials, 29, 1603885 (2017).

[30] T. Chiba, Y. Hayashi, H. Ebe, K. Hoshi, J. Sato, S. Sato, Y.-J. Pu, S. Ohisa, J. Kido, “Anion-exchange red perovskite quantum dots with ammonium iodine salts for highly efficient light-emitting devices,” Nature Photonics, 12, 681 (2018).

[31] M. Bruchez Jr., “Semiconductor Nanocrystals as Fluorescent Biological Labels,” Science, 281, 2013 (1998).

[32] J. M. Luther, J. Gao, M. T. Lloyd, O. E. Semonin, M. C. Beard, A. J. Nozik, “Stability Assessment on a 3% Bilayer PbS/ZnO Quantum Dot Heterojunction Solar Cell,” Advanced Materials, 22, 3704 (2010).

[33] M. Kulbak, D. Cahen, G. Hodes, “How Important Is the Organic Part of Lead Halide Perovskite Photovoltaic Cells? Efficient CsPbBr 3 Cells,” The Journal of Physical Chemistry Letters, 6, 2452 (2015).

[34] Y. Wang, X. Li, J. Song, L. Xiao, H. Zeng, H. Sun, “All-Inorganic Colloidal Perovskite Quantum Dots: A New Class of Lasing Materials with Favorable Characteristics,” Advanced Materials, 27, 7101 (2015).

[35] J. Chen, V. Hardev, J. Hartlove, J. Hofler, E. Lee, “66.1: Distinguised Paper : A High-Efficiency Wide-Color-Gamut Solid-State Backlight System for LCDs Using Quantum Dot Enhancement Film,” SID Symposium Digest of Technical Papers, 43, 895 (2012).

[36] Samsung Invests $11 Billion in Quantum Dot Display Manufacturing, https://www.nanosysinc.com/news/2019/10/10/samsung-invests-11-billion-in-quantum-dot-display-manufacturing (29 November 2019).

[37] K. P. Acharya, A. Titov, J. Hyvonen, C. Wang, J. Tokarz, P. H. Holloway, “High efficiency quantum dot light emitting diodes from positive aging,” Nanoscale, 9, 14451 (2017).

[38] L. Wang, J. Lin, Y. Hu, X. Guo, Y. Lv, Z. Tang, J. Zhao, Y. Fan, N. Zhang, Y. Wang, X. Liu, “Blue Quantum Dot Light-Emitting Diodes with High Electroluminescent Efficiency,” ACS Applied Materials & Interfaces, 9, 38755 (2017).

[39] B. S. Mashford, M. Stevenson, Z. Popovic, C. Hamilton, Z. Zhou, C. Breen, J. Steckel, V. Bulovic, M. Bawendi, S. Coe-Sullivan, P. T. Kazlas, “High-

efficiency quantum-dot light-emitting devices with enhanced charge injection," Nature Photonics, 7, 407 (2013).

[40] H.-M. Kim, J. Kim, J. Lee, J. Jang, "Inverted Quantum-Dot Light Emitting Diode Using Solution Processed p -Type WO x Doped PEDOT:PSS and Li Doped ZnO Charge Generation Layer," ACS Applied Materials & Interfaces, 7, 24592 (2015).

[41] X. Yang, E. Mutlugun, C. Dang, K. Dev, Y. Gao, S. T. Tan, X. W. Sun, H. V. Demir, "Highly Flexible, Electrically Driven, Top-Emitting, Quantum Dot Light-Emitting Stickers," ACS Nano, 8, 8224 (2014).

[42] Y. Yang, Y. Zheng, W. Cao, A. Titov, J. Hyvonen, J. R. Manders, J. Xue, P. H. Holloway, L. Qian, "High-efficiency light-emitting devices based on quantum dots with tailored nanostructures," Nature Photonics, 9, 259 (2015).

[43] H. Shen, W. Cao, N. T. Shewmon, C. Yang, L. S. Li, J. Xue, "High-Efficiency, Low Turn-on Voltage Blue-Violet Quantum-Dot-Based Light-Emitting Diodes," Nano Letters, 15, 1211 (2015).

[44] Y. Shirasaki, G. J. Supran, M. G. Bawendi, V. Bulović, "Emergence of colloidal quantum-dot light-emitting technologies," Nature Photonics, 7, 13 (2013).

[45] J.-H. Kim, K.-H. Lee, H.-D. Kang, B. Park, J. Y. Hwang, H. S. Jang, Y. R. Do, H. Yang, "Fabrication of a white electroluminescent device based on bilayered yellow and blue quantum dots," Nanoscale, 7, 5363 (2015).

[46] C.-Y. Han, K.-H. Lee, M.-S. Kim, J.-W. Shin, J. S. Kim, J.-H. Hwang, T. Kim, M. S. Oh, J. Kim, Y. R. Do, H. Yang, "Solution-processed fabrication of highly transparent mono- and tri-colored quantum dot-light-emitting diodes," Organic Electronics, 45, 145 (2017).

[47] W. K. Bae, J. Lim, D. Lee, M. Park, H. Lee, J. Kwak, K. Char, C. Lee, S. Lee, "R/G/B/Natural White Light Thin Colloidal Quantum Dot-Based Light-Emitting Devices," Advanced Materials, 26, 6387 (2014).

[48] J.-H. Kim, D.-Y. Jo, K.-H. Lee, E.-P. Jang, C.-Y. Han, J.-H. Jo, H. Yang, "White Electroluminescent Lighting Device Based on a Single Quantum Dot Emitter," Advanced Materials, 28, 5093 (2016).

[49] X. Yuan, J. Hua, R. Zeng, D. Zhu, W. Ji, P. Jing, X. Meng, J. Zhao, H. Li, "Efficient white light emitting diodes based on Cu-doped ZnInS/ZnS core/shell quantum dots," Nanotechnology, 25, 435202 (2014).

[50] H. Zhang, Q. Su, Y. Sun, S. Chen, "Efficient and Color Stable White Quantum-

Dot Light-Emitting Diodes with External Quantum Efficiency Over 23%," Advanced Optical Materials, 6, 1800354 (2018).

[51] M. K. Choi, J. Yang, K. Kang, D. C. Kim, C. Choi, C. Park, S. J. Kim, S. I. Chae, T.-H. Kim, J. H. Kim, T. Hyeon, D.-H. Kim, "Wearable red–green–blue quantum dot light-emitting diode array using high-resolution intaglio transfer printing," Nature Communications, 6, 7149 (2015).

[52] Q. Dai, C. E. Duty, M. Z. Hu, "Semiconductor-Nanocrystals-Based White Light-Emitting Diodes," Small, 6, 1577 (2010).

[53] X. Dai, Y. Deng, X. Peng, Y. Jin, "Quantum-Dot Light-Emitting Diodes for Large-Area Displays: Towards the Dawn of Commercialization," Advanced Materials, 29, 1607022 (2017).

[54] J. De Roo, M. Ibáñez, P. Geiregat, G. Nedelcu, W. Walravens, J. Maes, J. C. Martins, I. Van Driessche, M. V. Kovalenko, Z. Hens, "Highly Dynamic Ligand Binding and Light Absorption Coefficient of Cesium Lead Bromide Perovskite Nanocrystals," ACS Nano, 10, 2071 (2016).

[55] S. Dadı, Y. Altıntas, E. Beskazak, E. Mutlugun, "Plasmon Enhanced Emission of Perovskite Quantum Dot Films," MRS Advances, 3, 733 (2018).

[56] K.-H. Lee, J.-H. Lee, W.-S. Song, H. Ko, C. Lee, J.-H. Lee, H. Yang, "Highly Efficient, Color-Pure, Color-Stable Blue Quantum Dot Light-Emitting Devices," ACS Nano, 7, 7295 (2013).

[57] W. K. Bae, K. Char, H. Hur, S. Lee, "Single-Step Synthesis of Quantum Dots with Chemical Composition Gradients," Chemistry of Materials, 20, 531 (2008).

[58] W. K. Bae, J. Kwak, J. Lim, D. Lee, M. K. Nam, K. Char, C. Lee, S. Lee, "Multicolored Light-Emitting Diodes Based on All-Quantum-Dot Multilayer Films Using Layer-by-Layer Assembly Method," Nano Letters, 10, 2368 (2010).

[59] Y. Altıntas, M. Y. Talpur, M. Ünlü, E. Mutlugün, "Highly Efficient Cd-Free Alloyed Core/Shell Quantum Dots with Optimized Precursor Concentrations," The Journal of Physical Chemistry C, 120, 7885 (2016).

[60] Y. Altintas, A. Faruk Yazici, M. Unlu, S. Dadi, S. Genc, E. Mutlugun, "Excitonic interaction amongst InP/ZnS salt pellets," Journal of Materials Chemistry C, 5, 7328 (2017).

[61] M. D. Tessier, D. Dupont, K. De Nolf, J. De Roo, Z. Hens, "Economic and Size-Tunable Synthesis of InP/ZnE (E = S, Se) Colloidal Quantum Dots.," Chemistry of Materials, 27, 4893 (2015).